

**Potential Role of the Neural Stem Cell
Secretome in Modulating Neural Injury**

Carlos Rafael Faria Lopes

Thesis to obtain the Master of Science Degree in
Biomedical Engineering

Supervisor(s): Prof. Maria Margarida F. R. Diogo
and Prof. Susana Zeferino Solá da Cruz

Examination Committee

Chairperson: Prof. Claudia Alexandra Martins Lobato da Silva

Supervisor: Prof. Susana Zeferino Solá da Cruz

Members of the Committee: Prof. Sara Alves Xapelli

July 2021

*'And now the page before us blurs.
An age is done. The book must close.'*

- Steven Erikson

Acknowledgments

First and foremost, my thanks to Professor Susana Solá, for accepting me to the NSC Group, for the relentless support and for the incredible patience to put up with me for all this time. Your guidance kept my aim true and was the backbone of this entire venture. I would also like to extend my thanks to Professor Cecília for welcoming me to the Cellfun Group. Within the group, my gratitude goes first to Maria Ribeiro, for teaching me all I know about cell culture and just for always being available whenever something went wrong and to Sónia Sá Santos, who was also incredible, always ready with interesting insight and a calming word.

In parallel, I would like to thank Professor Joana Miranda, into whose laboratory I parachuted and that quickly became a second family within FFUL. Her expertise was instrumental in this work and I learned so much working there. In particular I have to thank Sérgio, tireless in his pursuit of both making sure I learnt 3D culture methods and did not break a propeller.

Finally my thanks to Professor Margarida Diogo, not only for accepting to be my internal supervisor but especially for being a great teacher throughout my Master's.

Tenho também de agradecer aos reféns, não só pelos almoços mas pelo apoio dentro e fora da sala de cultura. Especialmente ao João e à pequena Sónia, obrigado por ajudarem a manter a sanidade nos dias mais difíceis. Um obrigado também à Mafalda, por seres uma aluna tão interessada. Finalmente, um obrigado à Márcia pela amizade que se manteve apesar da distância.

Claro que tenho de agradecer ao famoso Jorge “Squarelord” Martins, pela amizade, não te livras de mim agora e à Carolina “Gaiata” Leitão, pela companhia e chamadas a caminho de casa. Não posso deixar passar também a amizade da malta das Caldas, Diogo e Nuno, isto já dura há algum tempo por isso vamos a mais uns quantos anos. Pela companhia aos cafés de sábado de manhã, um grande obrigado ao Rosário e Mykola, esperemos que o Raízes regresse. Deixo também uma palavra dedicada à Joana Ró, mas só uma porque sei que não és de muitas conversas. E claro, um grande obrigado ao grupo que me acompanhou ao longo do técnico, Anastasiya e Inês por partilharem o sofrimento das aulas práticas e trabalhos laboratoriais e Diana por seres a melhor madrinha que podia ter.

Finalmente, não podia deixar de agradecer à minha família, principalmente à minha mãe por sempre acreditar em mim, ao meu pai por me pressionar constantemente e às minhas irmãs por tudo.

A todos vós deixo os meus mais sinceros agradecimentos. Infelizmente não tenho veia de poeta que me permita exprimir quão agradecido estou, mas estes curtos parágrafos terão de servir.

Abstract

Neural stem cells (NSCs) are present in well-defined neurogenic niches of the adult mammalian brain, where they maintain the ability to self-renew and differentiate into new functional neural cells throughout life. Curiously, emerging evidence suggests that NSCs may also induce neural protection through their paracrine activity. Additionally, three-dimensional (3D) culture systems, which better resemble the *in vivo* physiology, have already been proven to enhance the cell secretome profile. Thus, the aim of this project was to explore the therapeutic potential of NSC-derived secretome in different *in vitro* models of neural damage and test the best culture system for improving the therapeutic properties of NSC-released factors. Initially, different *in vitro* models of neurodegeneration were established with NSCs and N2a with 1-methyl-4-phenylpyridinium (MPP⁺) and hydrogen peroxide (H₂O₂). Subsequently, for comparison of different culture NSC systems, a NSC spheroid culture model using Spinner flasks (3D system) was developed and validated with respect to spheroid formation and viability. However, the biochemical characterization of NSCs in 2D and the 3D culture systems, indicated that NSC spheroids present higher levels of neuronal differentiation markers when compared with the 2D system. Notably, 2D NSC-derived secretome was capable of rescuing cell viability in the models of neurodegeneration. Although not statistically significant, the assays demonstrated that 3D NSC-derived secretome also had an increased therapeutic value. Altogether, these results indicate that 2D is the better source of NSCs secretome, and more importantly, that NSC secretome present a therapeutic value which, in turn, can be improved in the future.

Keywords: Cell culture systems; Neurodegeneration; Neural stem cells; Secretome.

Resumo

As células estaminais neurais (NSCs) encontram-se no cérebro dos mamíferos adultos em nichos neurogênicos onde mantêm a capacidade de auto-replicação e diferenciação em novas células funcionais do sistema nervoso durante a vida do organismo. Curiosamente, estudos recentes sugerem que as NSCs podem induzir também a regeneração e proteção neural através da sua atividade parácrina. Adicionalmente, sistemas de cultura em três dimensões (3D), que representam melhor a fisiologia *in vivo*, têm revelado algumas melhorias nos perfis dos secretomas. Assim, o objetivo deste trabalho foi explorar o potencial terapêutico do secretoma produzido pelas NSCs em modelos de dano neural e investigar o sistema de cultura que resulta no secretoma mais protector. Inicialmente, diferentes modelos de neurodegeneração foram estabelecidos utilizando NSCs e N2a submetidas a 1-metil-4-fenilpiridina (MPP⁺) e peróxido de hidrogénio (H₂O₂). Subsequentemente, foi estabelecido e validado um modelo de cultura de NSCs em esferóides, de acordo com a formação e viabilidade dos esferóides. No entanto, quando comparados com o sistema 2D, os esferóides apresentaram níveis bastante mais elevados de marcadores de diferenciação. Finalmente, o secretoma proveniente das NSCs em sistema 2D induziu um aumento claro da viabilidade celular nos modelos de neurodegenerescência. Os nossos ensaios revelaram que o secretome obtido a partir de NSC em sistema 3D induz também uma resposta terapêutica. Em suma, os resultados indicaram que o sistema de cultura 2D é o mais adequado para a recolha de secretoma proveniente de NSCs e que o secretoma das NSCs possui propriedades terapêuticas, as quais poderão ser melhoradas no futuro.

Palavras-chave: Células estaminais neurais; Secretoma; Sistemas de cultura celular; Neurodegeneração.

Table of Contents

Acknowledgments.....	iv
Abstract	vi
Resumo	viii
Table of Contents.....	x
List of Figures	xii
List of Tables	xiv
List of Abbreviations.....	xv
1. Introduction	1
1.1. Stem cells.....	1
1.1.1. Neural Stem cells	3
1.2. Neurogenic niches	3
1.2.1. Regulation and maintenance of the neurogenic niches	6
1.3. Neurodegeneration	9
1.4. The paracrine hypothesis.....	13
1.5. Cell culture in three dimensions	16
1.6. Aims	18
2. Material and Methods.....	20
2.1. Ethics statement	20
2.2. 2D cell culture.....	20
2.2.1. Cells freezing and thawing.....	21
2.3. Viability assay.....	21
2.4. In vitro neural injury models	22
2.5. 3D cell culture.....	22
2.5.1. Cell aggregate measurement.....	23
2.5.2. Paraffinization of neurospheres	23
2.5.3. Haemotoxylin-eosin staining	24
2.6. Protein quantification	24
2.7. Secretome concentration	25
2.8. Total RNA extraction.....	25
2.9. qRT-PCR assay.....	26

2.10.	Immunocytochemistry	27
2.11.	NSC-derived CM-based assay	28
2.12.	Flow cytometry	28
2.13.	Statistical analysis	29
3.	Results and Discussion	30
3.1.	Optimization of in vitro injury models in mouse neural stem cells and neural cells	30
3.2.	Effect of NSC-derived secretome on MPP+ and H2O2-induced NSC death.....	33
3.3.	Establishment of the NSC three-dimensional culture system for collection of NSC secretome	35
3.4.	Comparison of the therapeutic impact of NSC secretome derived from 2D and 3D culture conditions	38
3.5.	Molecular characterization of 2D- and 3D-derived NSCs	43
3.6.	Molecular characterization of NSC secretome-receiving cells	48
4.	Conclusions and Future Perspectives.....	51
5.	References	53

List of Figures

Figure 1 – The anatomy of neurogenic niches in the adult mouse brain.	5
Figure 2 – Potential effects of α -syn aggregation in PD.	10
Figure 3 – Mitochondrial dysfunction in PD.	11
Figure 4 – Changes in the secretome produced by human NSC after being grafted into rodent models of neurodegeneration.	14
Figure 5 – Key aspects of 3D culture.	17
Figure 6 – Schematic of the protocol described for 3D culture of NSCs in spinner flasks	23
Figure 7 – MPP ⁺ and H ₂ O ₂ decrease cell viability in NSCs.	31
Figure 8 – MPP ⁺ and H ₂ O ₂ show virtually no effect on cell viability in differentiating NSCs.	31
Figure 9 – MPP ⁺ and H ₂ O ₂ show a decrease in cell viability in N2a cells.	32
Figure 10 – Supplementation of media with CM increases viability in injury models.	34
Figure 11 – The addition of CM induces protection in NSC injury models.	35
Figure 12 – Representative images of aggregates grown in ULA plates.	36
Figure 13 – Diameter of NSC spheroids increases during culture.	37
Figure 14 – Larger spheroids associated with higher initial cell density exhibit necrotic centres, whereas smaller spheroids associated with lower initial cell density are homogenous.	38
Figure 15 – Supplementation of NSC media with CM improves live cell count in NSC injury models.	40
Figure 16 – Supplementation of N2a media with CM improves live cell count in H ₂ O ₂ injury model.	42
Figure 17 – Gene expression evaluated with qPCR reveals increased differentiation on 3D cultured NSCs.	45
Figure 18 – Gene expression evaluated with qPCR reveals increased mitochondrial activity on 3D cultured NSCs.	46
Figure 19 – Immunostaining of spheroids reveals the expression of genes on the aggregate. .	48
Figure 20 – Flow cytometry reveals no appreciable change in Bcl-2 expression following administration of CM in N2a injury model.	49

List of Tables

Table 1 – List of primers used for qRT-PCR	26
Table 2 – List of primary antibodies used for immunohistochemistry.....	27
Table 3 – List of secondary antibodies used for immunohistochemistry	28

List of Abbreviations

2D	Two dimensions
3D	Three dimensions
BBB	Blood brain barrier
BDNF	Brain derived neurotrophic factor
CM	Conditioned media
CNTF	Ciliary neurotrophic factor
CSF	Cerebrospinal fluid
DG	Dentate gyrus
ECM	Extracellular matrix
ESC	Embryonic stem cell
EZ	Ependymal zone
FBS	Fetal bovine serum
FC	Flow cytometry
FM	Fresh media
GCL	Granular cell layer
GDF11	Growth differentiation factor 11
IGF	Insulin-like growth factor
IGFBP6	Insulin-like growth factor binding protein 6
I- γ	Interferon γ
IL-4	Interleukin-4
iPSC	induced pluripotent stem cell
LB	Lewy's bodies
LV	Lateral ventricles
ML	Molecular layer
MPP ⁺	1-methyl-4-phenylpyridinium
MPTP	1-methyl-4-phenyl-1,2,3,6-tetrahydropyridine
MSC	Mesenchymal stem cells
NGF	Nerve growth factor
NSC	Neural stem cell
NT-3	Neurotrophin-3
OB	Olfactory bulb
PD	Parkinson's disease
PEDF	Pigment endothelium-derived factor
qRT-PCR	Quantitative reverse transcriptase polymerase chain reaction
ROS	Reactive oxygen species
SC	Stem cell
SGZ	Sub granular zone
SN-pc	<i>Substantia nigra pars compacta</i>

SVZ	Sub ventricular zone
TGF- β	Transforming growth factor β
UPS	Ubiquitin proteasome system
ULA	Ultra-low attachment
VEGF	Vascular endothelial growth factor
α -syn	α -synuclein

1. Introduction

First hinted at by the experiments of McColluch and Till [1] in the form of haematopoietic progenitors, stem cells have captured the imagination of the scientific community with their apparent limitless potential ever since. Experiments and applications have been designed, countless scientific papers have been written, however with the exception of bone marrow transplants, therapies using stem cells have been largely unsuccessful. This led to another avenue of scientific exploration. Instead of directly using stem cells, could the secretome, the collection of growth factors, cytokines, microRNAs (miRNAs) and other metabolites secreted by these cells, be harnessed for therapeutic ends?

1.1. Stem cells

Stem cells are recognised to possess two defining characteristics, namely self-renewal, which is the ability to proliferate while maintaining their characteristics, and potency, the ability to differentiate into more specialised cells [2]. Stem cell self-renewal is powered by two different processes of cell division. Symmetrical cell division results in two identical daughter-cells and it is essential in early development to establish a pool of stem cells which will give rise to tissue. At a certain point, however, the dominant cell division process becomes asymmetrical giving rise to two cells with different levels of potency. In particular this provides a cell with equivalent potency to the original cell and one committed to a specific fate, maintaining the stem cell pool and creating new cells at the same time [3].

The potency of a particular population of stem cells can be used to classify cells, namely, by how broad a range of different cell types can be originated from a stem cell. Totipotency, the property exhibited by the zygote and subsequent cells up until the fourth day after fertilization represents the highest level of potency, when a single stem cell is capable of originating not only all cells of the organism, but also cells found in supporting structures of the fetus, namely the trophoblast, which eventually originates the trophoderm and then the placenta. After developing the trophoblast, the Inner Cell Mass exhibits pluripotency, the ability to generate cells from all three germ layers (Endoderm, Mesoderm and Ectoderm). While capable of originating all the cells of the organism, they require the support provided by the trophoblast to actually generate the fetus. Multipotency is further restricted in terms of differentiation, being confined to cells belonging to one germ layer. Oligopotency, in turn, is defined by the ability to differentiate into a subset of cells belonging to the same germ layer. Lastly, unipotent cells can only originate one type of cell [4]. Of note, this classification exists in a continuum and decreasing order of potency, from totipotency, pluripotency, multipotency, oligopotency and unipotency, leading to a certain blurring of the lines in some recently discovered cell types. As an example, Neuromesodermal progenitors appear to be capable of differentiation into two germ layers, which would place them somewhere between pluripotent and multipotent cells [5, 6].

Moreover, stem cells can also be classified according to their point of origin. Indeed, their potency can also be correlated with the point in the development of the organism that they are isolated, with reduced potency as development progresses. Embryonic stem cells (ESCs) are derived from the inner cell mass and are pluripotent. Fetal stem cells are isolated from fetal or extra-fetal tissue and can range between pluripotent and multipotent. Neonatal stem cells are derived from the umbilical cord blood and are merely multipotent. Some authors make no distinction, encasing neonatal stem cells in the fetal stem cell classification [7]. In the adult organism, stem cells can be isolated from almost every tissue. These adult stem cells can range in potency from multipotent to unipotent. Finally, induced pluripotent stem cells (iPSCs) are stem cells obtained from somatic cells. In this case, an adult differentiated cell undergoes reprogramming and returns to an undifferentiated state. Similar in potency to ESCs, iPSCs were initially generated with the inclusion of four transcription factors [8]. Recently, however, iPSCs were obtained using small molecules, using a simpler and more reproducible protocol [9].

1.1.1. Neural Stem cells

Neural stem cells (NSCs) are a type of multipotent stem cell capable of differentiating into neurons, astrocytes and oligodendrocytes. They are first found in the neuroectoderm, a subset of the ectoderm in the embryo that will eventually become the entirety of the nervous system. However, some populations of NSCs will maintain their potency, albeit in a quiescent state, during the adult life of the organism. Located in neurogenic niches, these cells can be activated by a myriad of factors, leaving the quiescent state to return to the cell cycle. Once activated, they can undergo symmetrical divisions, increasing the pool of NSCs or asymmetrical divisions which results in one cell of each type [10].

1.2. Neurogenic niches

In the adult mammalian brain, NSCs are mainly found in two different niches, the Subventricular Zone (SVZ) located on the outer walls of the two Lateral Ventricles (LV) and the Subgranular Zone (SGZ) located in the Dentate Gyrus (DG) of the hippocampus. These populations appear different *in vivo*, with the SVZ population giving rise to both olfactory bulb (OB) interneurons and *corpus callosum* oligodendrocytes. Furthermore, this cell population varies along depending on the location within the SVZ, considering that ventral located NSCs generate deep granule cells and calbindin-expressing periglomerular cells, while dorsal located cells generate instead superficial granule cells and tyrosine hydroxylase-expressing periglomerular cells. The SGZ cells, in turn, generate dentate granule neurons and astrocytes [10]. Nonetheless, *in vitro* assays have confirmed the potency of these cells, in which both populations have been differentiated into all three neural lines with the appropriate protocols, suggesting that the interplay between the NSCs and their niche is responsible for guiding their respective differentiation pathways [11].

One important aspect is also the fact that the blood brain barrier (BBB) is more porous near the neurogenic niches, facilitating the access to blood-borne factors [12]. Two of these factors, the vascular endothelial growth factor (VEGF) and the neurotrophin-3 (NT-3) are secreted by endothelial cells and found circulating in the blood and the Cerebrospinal Fluid (CSF). When up taken by NSCs, they promote self-renewal and quiescence respectively [13].

The ventricular space is lined with ependymal cells. This ependymal zone (EZ), separates the ventricular space from the SVZ, the region where the adult NSCs reside. This population of NSCs, also known as type B cells, and are kept in a quiescent state until the deemed necessary time to give rise to transient amplifying progenitors (also known as type C cells). Type C cells proliferate and give rise to neuroblasts (type A cells). Type A cells will then follow the rostral migratory stream, reaching the OB, where they will further differentiate into granule cell interneurons or periglomerular cell interneurons. Once fully mature, it is suspected that these cells will play an important part in learning associated with odour recognition. During the differentiation and migratory process, cells will interact differently with the extracellular matrix (ECM), particularly with a layer rich in proteins belonging to the family of laminins [11]. Morphologically, Type B cells have their cell body located in the SVZ, however they display two processes, or neurites, in opposing directions. The basal neurite reaches the blood vessels that are found in the SVZ, and the apical one reaches across the EZ, through the ependymal rosettes and into the CSF found in the ventricle. In primates, as well as humans, the SVZ has an extra layer, mainly composed of extensions from the ependymal cells and astrocytes, with few cell bodies [14]. Furthermore, while neuroblasts in rodents follow the rostral migratory stream, in humans the stream seems to follow a lateral ventricular extension [15].

The NSC population found in the SGZ, also known as Type 1 Cells or radial glia-like cells, is found between the Hilus and the Granular Cell Layer (GCL), with a neurite that extends through the GCL and into the Molecular Layer (ML). Type 1 cells differentiate into transit-amplifying non-radial progenitor cells (Type 2a Cells), which in turn originate intermediate progenitor cells (Type 2b Cells), that subsequently give rise to neuroblasts (Type 3 Cells). Type 3 Cells will then migrate to the GCL and differentiate into dentate granular neurons. This ongoing adult neurogenesis contributes to the neuroplasticity observed in the DG and is believed to be relevant for memory formation [16].

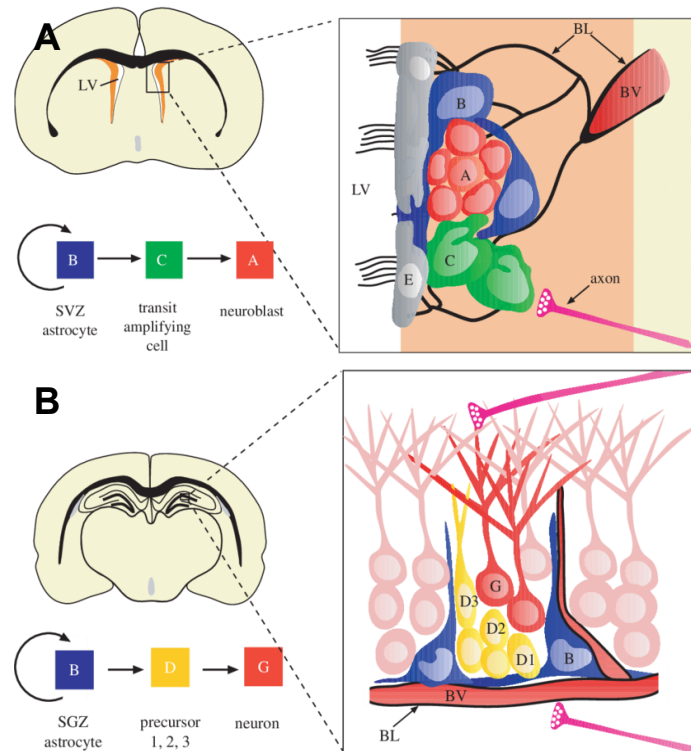


Figure 1 – The anatomy of neurogenic niches in the adult mouse brain. (A) on the left, a coronal section of the brain, with the SVZ highlighted in orange, by the LV, and the differentiation pathway from NSC to neuroblasts. On the right, the structure of the SVZ is expanded, revealing the interactions between the different cell types (A, red: Type A Cell; B, blue: Type B Cells; C, green: Type C Cell; E, grey: Ependymal cells) as well as blood vessels (BV) and basal lamina (BL) a specialised extracellular matrix. (B) on the left a coronal section of the brain and the differentiation pathway from NSC to neurons. On the right, the structure of the SGZ is expanded, again highlight the interactions between the different cell types (B, blue: Type 1 Cells; D1/D2/D3, yellow: intermediate progenitor cells; G, red: neurons) and the blood vessel. Adapted from [17].

1.2.1. Regulation and maintenance of the neurogenic niches

Regarding the complexity of both neurogenic niches, they are expected to be tightly regulated by both extrinsic and intrinsic factors. Intrinsic factors are considered part of the niche, including cells, matrix and all interactions *in situ* by proximity with the NSCs. Extrinsic factors, in turn, arise from other parts of the organism. This combined interplay is essential to keep stem cells in the potent state and to induce differentiation when required, being the key to understand neurogenesis and the role that the cell secretome might play [18].

One of these factors is the presence of astrocytes in the neurogenic niche, which in turn may trigger different mechanisms of action to induce or inhibit NSC differentiation. As an example, through juxtacrine interactions, astrocytes can inhibit neurogenesis via the Jagged1-mediated Notch pathway. Moreover, astrocytes also display paracrine activity, being capable of secreting

factors such as insulin-like growth factor binding protein 6 (IGFBP6) and decorin which also inhibit the differentiation of NSCs. However, astrocytes can also induce neurogenesis through their juxtacrine and paracrine activity. Namely, cell-to-cell contacts with astrocytes exhibiting Ephrin-B2 was shown to promote differentiation in the SGZ through the upregulation of the EphB4 receptor-mediated pro-neuronal transcription factor [19], while the secreted factors such as Wnt3, Neurogenesis-1 and Thrombospondin were also shown to increase neurogenesis [18].

Regarding microglia, they couple their regulatory potential with a more direct approach to maintain niche homeostasis [20]. Microglia are the brain immune cells, responsible for phagocytosis in the central nervous system (CNS). The removal of apoptotic cells before they can turn into secondary necrotic cells protects the surrounding cells from the release of proinflammatory cellular contents. In particular, the majority of new-born Type 3 Cells found in the SGZ region undergo apoptosis, instead of further differentiating, and are phagocytosed by microglia cells in this same niche [21]. Additionally, microglia also display paracrine activity. Increased levels of transforming growth factor β (TGF β) and nerve growth factor (NGF), which inhibit and promote neurogenesis respectively, are secreted following the phagocytosis process [22]. Furthermore, when microglia are stimulated *in vitro* with interleukin-4 (IL-4) and interferon- γ (I- γ), they promote neurogenesis through the secretion of insulin-like growth factor 1 (IGF-1) [23]. In fact, in *in vivo* rat models of stroke, microglia were shown to induce neurogenesis using the same pathway of IGF-1 [24].

On the other hand, the endothelial cells that form the blood vessels which border the niches, as well as the pericytes found in close contact, also exhibit paracrine activity, possibly influencing neurogenesis [25]. The secretion of VEGF by endothelial cells, induces not only angiogenesis [26], but also neurogenesis in both niches [17, 27], being key in neurogenesis mediated by exercise [28]. Endothelial cells also produce brain derived neurotrophic factor (BDNF) which protects NSCs from injury [29] and enhances survival of newly formed neurons [30]. BDNF is also produced in hypoxia conditions to promote angiogenesis [31], and most importantly, BDNF promotes neurogenesis in the OB region, along the rostral migratory stream [32]. Pericytes also secrete BDNF under normal conditions, while when under hypoxia conditions the NT-3 expression is upregulated, leading to NGF secretion by the astrocytes [33].

Curiously, unlike in astrocytes, the expression of the Ephrin-B2 receptor in combination with Jagged1 in endothelial cells is linked to the maintenance of NSC quiescent state in SVZ [34]. In the SVZ, ependymal cells are found lining the ventricles, where their cilia contribute to the flow of the CSF [35]. Indeed, they secrete the pigment epithelium-derived factor (PEDF) capable of promoting self-renewal of Type B Cells [36]. In the absence of ependymal cells, a condition closely associated with pathological conditions [37, 38], it has been shown that neurogenesis is greatly impaired [38]. Interestingly, and as another example of cellular interplay in the neurogenic niches, when the ependymal cell layer is damaged, astrocytes can replace ependymal cells and take on some properties of these missing cells [39].

Beyond these intrinsic factors, some factors originate from outside, reaching the neurogenic niches through several pathways. One example is by the vasculature that borders the niches.

Prolactin, a protein secreted in the hypophysis, functions as a hormone to promote neurogenesis in the SVZ, mainly during pregnancy [40]. On the other hand, glucocorticoids produced as part of the stress response inhibit neurogenesis [41, 42]. In one particular model, the neurodegenerative effects of aging in neurogenic niches were averted by the effect of blood-borne factors associated with youth, including growth differentiation factor 11 (GDF11). This study showed increased neurogenesis and angiogenesis [43].

Importantly, the other fluid that is in contact with a neurogenic niche is the CSF, found in the ventricles by the SVZ. Akin to the migration of neuroblasts found in the SVZ, the CSF flows from the choroid plexus, the main source of CSF, in parallel to the rostral migratory stream. In fact, since the ependymal cells are essential for the correct flow of CSF in the ventricle, their absence causes impairment of the flow and disturbance of the neuroblasts' migratory pathway [44]. Furthermore, the composition of the CSF is also crucial for the maintenance of the SVZ niche. For example, the presence of IGF-1 in CSF promotes proliferation and migration of neuroblasts [45], while ciliary neurotrophic factor (CNTF) is involved in the self-renewal of NSCs [46] and sphingosine-1-phosphate induces NSC quiescence [47].

Recently, the neurogenic niches were also shown to be regulated by neurotransmitters. Despite the lack of traditional synapses associated with neurotransmitter signalling, NSCs can be stimulated by neurotransmitters through tonic activation [48]. In fact, dopaminergic neurons in the *Substantia Nigra pars compacta* (SN-*pc*) extend dendrites to the SVZ, where NSCs expressing dopamine receptors can also be found. The role of dopamine in the SVZ-associated NSCs was first suggested when the ablation of dopaminergic neurons resulted in markedly decreased neurogenesis [49]. Then, the delivery of dopamine receptor agonists was shown to rescue the impaired neurogenesis, confirming this same hypothesis [50]. Interestingly, a similar study shows decreased NSC proliferation in the SGZ and subsequent recovery when the serotonergic neurons, which have projections into the DG, were removed and then replaced via graft [51, 52]. The DG has also projections of noradrenergic neurons located in the *locus coeruleus*, and the administration of either noradrenaline reuptake inhibitor, which in turn leads to increased extracellular levels of noradrenaline, or β_3 -adrenergic receptor agonist, leads to increased proliferation [53, 54]. On the other hand, ablation of the same neuron population leads to decreased proliferation on the SGZ [55].

However, none of the aforementioned regulatory pathways exist in a vacuum. Instead they are constantly interacting *in vivo* in order to maintain homeostasis. Two such systems that interact are the serotonin mediated proliferation [30] and the BDNF pathway which improves the long-term survival of newly differentiated neurons in the SGZ [30] as well as differentiation and maturation [56]. However, when a serotonin reuptake inhibitor is administered simultaneously to the blocking of the BDNF receptor p75, despite an increase in NSC proliferation, no net gain was observed in the number of neurons [57]. However, if the BDNF receptor *trkB* is blocked, the entire serotonin-induced response is inhibited, further highlighting how closely related the pathways are [58].

1.3. Neurodegeneration

Neurodegenerative diseases are a type of disorders characterised by the selective loss of a subset of neural cells. The second most prevalent of which is Parkinson's Disease (PD) [59], which is characterized by the loss of dopaminergic neurons in the SN-pc [60]. PD is a very heterogenous disorder [61], and patients exhibit a range of symptoms, broadly categorized as motor, such as bradykinesia and tremor, cognitive and psychiatric, which also entails depression and apathy among others [62]. At the molecular and cellular level, PD is characterized by the increased expression and misfolding of α -synuclein (α -syn) [63], a protein associated with synaptic activity [64], which then aggregates into β -sheet rich fibrillar amyloid fibrils [65]. The amyloid fibrils aggregate in turn, forming Lewy Bodies (LB) [66]. Considering that the amyloid fibrils are toxic [67], there is evidence that LB may act as a neuroprotective device [68]. However, since LB can also fragment into the more toxic oligomers, this is as of yet unclear [69].

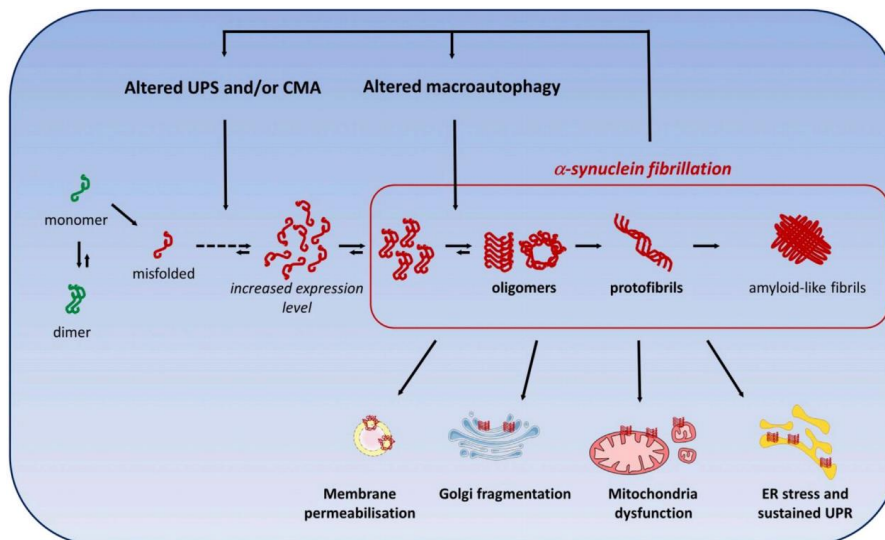


Figure 2 – Potential effects of α -syn aggregation in PD. The misfolded form of the protein aggregates into dimers and then into oligomers, stabilised by β -sheet like interactions. The protofibril stage is insoluble and leads to further aggregation into the amyloid-like fibrils and the typical LB. The aggregation of the different structures is facilitated by alterations in the ubiquitin proteasome system (UPS) or the chaperone-mediated autophagy (CMA) degradation pathways, for single proteins, whereas changes in macroautophagy would result in accumulation of the various aggregates. Moreover, the different types of aggregates appear to have different toxicity pathways, affecting different organelles. Adapted from [70].

The specific pathway for cytotoxicity of the α -syn fibrils is a matter of discussion, as several pathways have been proposed [70]. Of particular interest to this work is the effect of PD in mitochondrial activity, since the model studied relies upon the inhibition of the mitochondrial complex I through the administration of 1-methyl-4-phenylpyridinium (MPP⁺) [71]. The link between mitochondrial activity and PD was witnessed when autopsies of PD patients revealed a

decrease in the activity of mitochondrial complex I [72] and confirmed by a previous study of the symptoms caused by the accidental injection of 1-methyl-4-phenyl-1,2,3,6-tetrahydropyridine (MPTP), a prodrug of MPP⁺, which resembled sporadic Parkinsonism [73]. Furthermore, genes associated with PD, namely PINK1 and *parkin* are involved in the proper functioning of the mitochondria [74, 75], as well as promoting the mitophagy of damaged mitochondria [76] whereas patients with PD exhibit damaged mitochondria [77]. Similarly altered mitochondria are seen on MPP⁺ models [78] as well as in models with overexpression and accumulation of α -syn [79]. On the other hand, activation of PINK1 and *parkin* reverted the changes to mitochondria [80], again highlighting the connection between PD and mitochondria and also suggesting a potential target for therapeutics.

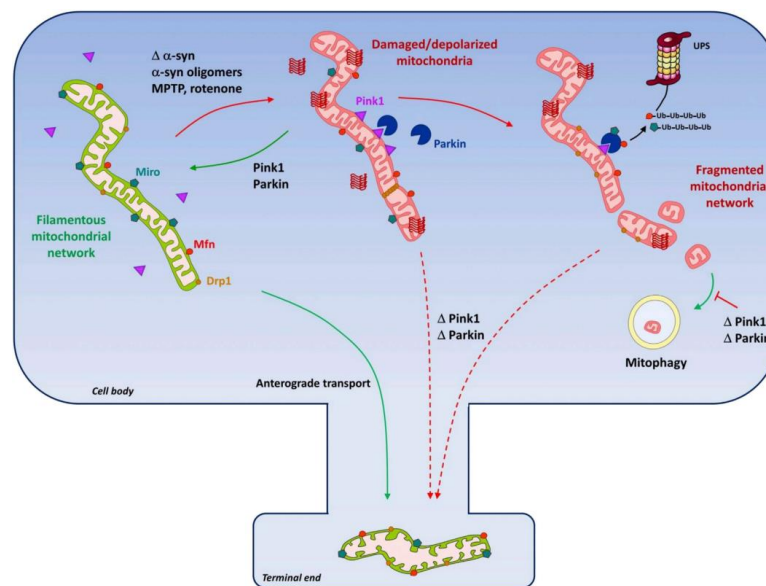


Figure 3 – Mitochondrial dysfunction in PD. The accumulation of oligomers of α -syn induces mitochondrial fragmentation. This effect is also seen in MPP⁺ related injury and oxidative stress. Recent studies suggest that PINK1 and *parkin* are responsible for the mitophagy of damaged mitochondria. Specifically, damaged mitochondria recruit PINK1 on the outer membrane, which in turn recruits *parkin*, an ubiquitin ligase that activates the UPS-dependent degradation pathway. The fragments are then further degraded in lysosomes. Thus, mutations in PINK1 or *parkin* may impair mitophagy and contribute to the accumulation of dysfunctional mitochondria, skewing the dynamics of mitochondria activity. Adapted from [70].

Considering the localized injury observed in the PD patients, regenerative medicine was considered a viable therapeutic method. One initial treatment consisted of grafts of fetal derived dopaminergic neurons to the *putamen* of a patient with severe sporadic PD. This resulted in a marked recovery of the motor symptoms, such as rigidity that characterises PD [81]. However recent reviews showed that the therapeutic outcome of grafts depends on more than mere volume of dopaminergic neurons grafted, such as on the neural survival and integration levels [82].

Moreover, the ethical concerns associated with fetal tissue difficult the obtention of the necessary cell mass. A single graft requires several embryos, due to the limited expandability of stem cells [83]. To circumvent that issue, dopaminergic neurons were differentiated from ESC and implanted in a MPTP monkey model, showing improved neurological symptoms [84]. Another study, using the same monkey model, revealed that grafted NSC of human origin can differentiate *in vivo* without external cues, ultimately ameliorating the motor symptoms of PD [85].

Regarding the ethical concerns, dopaminergic neurons can be obtained from reprogrammed fibroblasts, bypassing the need for embryonic or fetal tissue. These cells, when grafted in a different PD rat model, induced motor recovery [86]. In fact, animals that showed recovery were later found to present cells positive for tyrosine hydroxylase, an enzyme that hydroxylates a precursor for dopamine, as well as fibres that extended outside of the graft [86]. The use of iPSCs can also bypass the rejection problem of allogenic grafts, since the grafted cells can be sourced from the very patient [87]. On the other hand, the genetic stability of iPSCs is unclear, with recent studies suggesting that iPSCs are less stable and more prone to mutations and epigenetic alterations [88].

Regardless of the cell source, the transplantation of stem cells entails the risk of teratoma formation, or uncontrolled growth of immature proliferative neural precursors. Even through selection of differentiated cells, it is possible for a few stem cells to evade detection and originate a teratoma, requiring more complex methods to ensure the safety of a graft [89]. The risk can also be decreased by increased maturation of the cells. However, more mature cells show decreased survivability in grafts [90], which would require that a delicate balance be achieved.

1.4. The paracrine hypothesis

The largely unfulfilled regenerative potential of stem cell grafts leads to the exploration of the *paracrine hypothesis*, according to which stem cells can ameliorate the symptoms of chronic inflammation not only through cell replacement, but also through the secretion of growth factors and other components of their secretome [91].

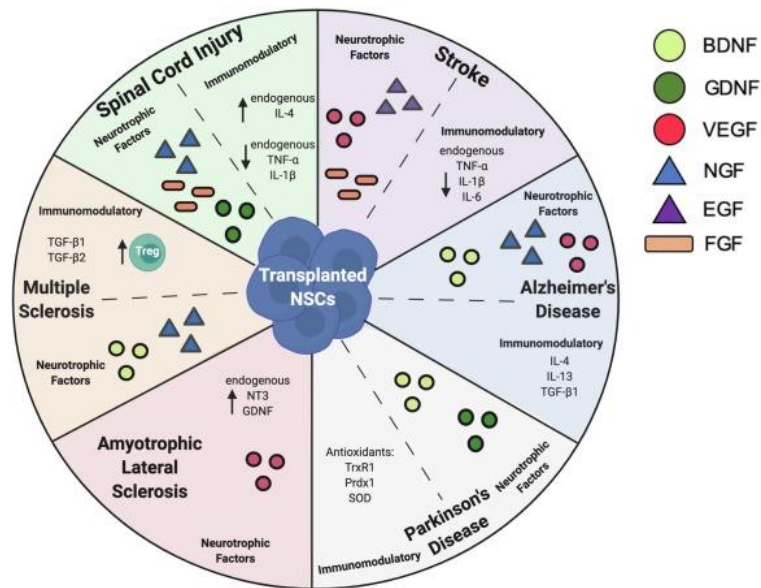


Figure 4 – Changes in the secretome produced by human NSC after being grafted into rodent models of neurodegeneration. Up arrow (↑) indicates an increase; down arrow (↓) indicates a decrease. Adapted from [92].

Early evidence of the paracrine hypothesis was found when injection of bone marrow derived mesenchymal stem cells (MSC) in a mice model of autoimmune encephalomyelitis resulted in a significant improvement [93]. Considering that MSCs do not differentiate into neuronal tissue, outside of artificial conditions of transdifferentiation, the results indicated that the protective mechanism did not rely on replacement of the lost tissue. *In vitro* experiments showed similar results when MSCs were co-cultured in contact with dorsal root ganglia post mitotic sensory neurons. In this study, the neurons were also able survive and mature further when co-cultured compared with other cell types [94]. Another *in vivo* assay of injection of MSCs resulted in increased neurogenesis and migration of increasingly mature neurons. Here, the expression of growth factors such as NGF, VEGF and CNTF significantly increased, however it was not clear whether these growth factors were expressed directly by the MSCs or indirectly through the activity of astrocytes [95]. In addition, the expression of BDNF in specific MSC populations was also correlated with survivability in a neuroblastoma cell line when co-cultured with MSCs [96].

Similar experiments using NSCs showed the same results, grafts of SVZ-derived NSCs in PD mice models ameliorated motor symptoms but resulted in reduced effective regeneration of tissue [97, 98]. In order to study the effect of the secretome without the influence of the cells themselves, either through integration of cells or mechanical cues, it became imperative to isolate the secretome from the NSCs. For that, cells were plated and the culture media collected. This culture media is conditioned by the presence of cells and contains the components of their secretome. Notably, the administration of this culture media induced a significant recovery of motor function and increased tyrosine hydroxylase expression when compared with simple NSC

grafts [99]. This method has other more practical advantages facing grafts. Besides the ease of production, when we think in terms of obtaining and expanding a prohibitively large cellular count, the secretome also avoids compatibility issues, since it is cell free and incurs no risk of rejection [92].

Having ascertained the protective effect of stem cell secretome, several approaches can be used to further refine its effectiveness. One approach consists of an initial proteomic analysis of the secretome to induce overexpression of components which may improve its protective profile. Interestingly, this approach has been successfully studied in a PD mice model, using the secretome of astrocytes with increased expression of Glial cell-derived neurotrophic factor [100]. Another approach consists on the pre-conditioning of secretome producing cells with a mild form of damage, such as hypoxia, to stimulate the protective effect in response of the cells to injury [101]. Taken together, the objective has been to obtain the best possible secretome to respond to injury or damage, either through a broad scope effect or a more specialized one.

1.5. Cell culture in three dimensions

Stem cells are commonly cultured in two dimensions (2D), as a monolayer adherent to the surface of the culture flask. There are some advantages to this methodology, namely the straightforward control of the culture conditions and the reproducibility. Since the cells are equally distributed across the surface and submerged in medium, the concentration of nutrients and growth factors will be equal and all the cells will be kept in similar conditions of stemness [102]. However monolayer culture is not a good simulacrum for physiological tissue [103]. Cells in monolayer culture lack a supporting extracellular matrix (ECM) structure and the associated biomechanical cues [104]. Furthermore, cells in 2D exhibit alterations of the cytoskeleton which in turns affects gene expression [105]. It should be considered, however, that 3D culture systems are much more expensive and complex than traditional 2D culture and exhibit greater variability [106].

In order to improve cellular models, culture in 3D was introduced. There are different methodologies for 3D culture, depending on the presence or absence of a biomaterial scaffold [107]. The simplest method is the aggregation of cells in suspension, creating spheroids [108]. Spheroids are roughly spherical in shape and thus, a gradient of nutrients, growth factors and oxygen is formed along the axis of the structure. This gradient results in a very heterogeneous population of cells, in varying states of differentiation. However, if allowed to grow disproportionately, spheroids are unable to adequately transfer nutrients and oxygen, resulting in necrotic centres [109]. Thus, establishing a proper protocol for 3D culture requires optimization. Moreover, a protocol is not typically transferable across the various possible techniques to culture spheroids, which range from hanging drop and the usage of ultra-low attachment plates to spinner flasks and bioreactors, requiring further optimization [106]. Furthermore, cells cultured as spheroids exhibit a behaviour similar to that of *in vivo* cells, making them a more suitable model for drug testing and disease modelling [110].

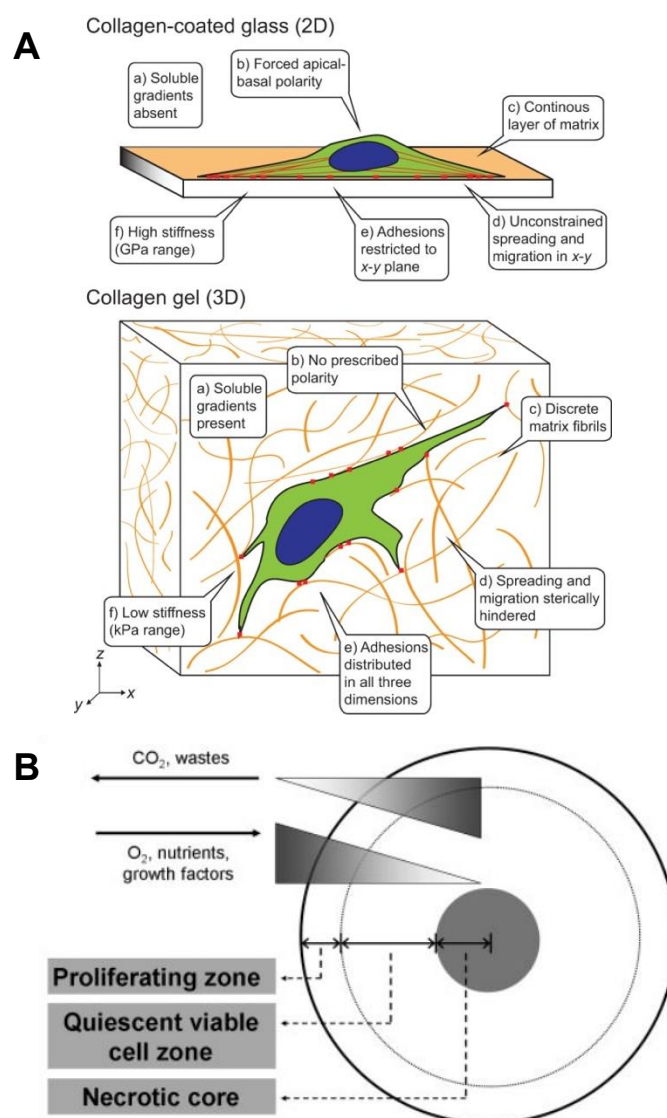


Figure 5 – Key aspects of 3D culture. A - Difference in cues (adhesive, topographical, mechanical and soluble) encountered by cells cultured in traditional 2D culturing surface and a 3D culturing method (a collagen ECM in a gel). Adapted from [111]. **B** - Schematic of the gradients found along the radius of a cell spheroid. The different zones found along the same axis are a function of the gradients the cells encounter in this microenvironment. Adapted from [112].

Nonetheless, when it came to modelling tissues, spheroids were found to still be lacking in both complexity and organization of cells. Indeed, even animal models were unable to properly replicate neurodevelopmental and neuropsychiatric disorders. However, recent experiments showed the remarkable capability of stem cells to self-organize and replicate the embryonic development [113, 114]. Since then, different protocols for the generation of the so-called organoids, have been developed, allowing the generation of more complex tissue, sometimes

with added support provided with an artificial scaffold [115]. The incredible potential behind organoids was immediately apparent when it became possible to simulate microcephaly to a greater extent than animal models, due to the anatomical differences between rodents and humans [116]. The study of organoids has led increasingly better recapitulation of *in vivo* development, which is key for studies in the field of developmental biology and disorders associated with development [115]. Recent developments in the field lead to the generation of organoids which exhibit not only cells from different germ layers, but also functional neuronal circuits [117]. Despite the inherent difficulties, the advantages of 3D culture far surpass the disadvantages, and it should be seen as a promising strategy for furthering research across several fields.

1.6. Aims

Based on the possibility to strategically modulate NSC secretome and, therefore, better respond to neural damage, we aimed to:

1. Evaluate the potentially protective effect of NSCs secretome on *in vitro* models of Parkinsonism and neural oxidative stress.
2. Perform a 2D and 3D cell culture comparison to offer the best protective effect of the NSC secretome.
3. Perform a 2D and 3D cell culture comparison to provide a homogenous NSC population for molecular biology studies and future manipulation of the secretome.

A further clarification of the impact of NSC secretome in neighbouring damaged cells as well as the best-defined culture system to therapeutically improve this secretome will certainly accelerate the investigation and effectiveness of this emerging area of research. This study improves our understanding on which culture system should NSCs be maintained to ensure the harvest of naïve NSC-derived secretome and, at the same time, investigate the molecular mechanisms associated with those secretome for a pharmacological modulation in a near future.

2. Material and Methods

2.1. Ethics statement

The mouse NSC line NS-TGFP used in this study was obtained from Dr. Smith's Laboratory, University of Cambridge, Cambridge, UK and provided by Dr. Henrique, Faculty of Medicine, University of Lisbon, Lisbon, Portugal. The Neuro2a cell line (N2a) was purchased and provided by Dr. Andreia Carvalho, Research Institute for Medicines (iMed.Ulisboa), Faculty of Pharmacy, University. The Animal Ethical Committee at the Faculty of Pharmacy, University of Lisbon, Portugal waived the need for approval.

2.2. 2D cell culture

In 2D culture system, NSCs were cultured in a monolayer and passaged after reaching 80% confluency. For that, cells NSCs were washed with 4 mL of Phosphate Buffered Saline (PBS) and incubated 3 min with 1 mL of Accutase (A11105-01; Gibco™) at 37°C. After dissociation from the culture dish, 2 mL of PBS was added to dilute the Accutase enzyme. NSCs were then collected and centrifuged at 500 *g* for 5 minutes. After discarding the supernatant, the cell pellet was resuspended in freshly prepared medium. The medium used was Euromed-N (EuroClone S.p.A., Pavia, Italy) supplemented with 1% of both N-2 supplement (Gibco, Thermo Fisher Scientific, Inc., USA) and Penicillin-Streptomycin (P/S, Gibco, Thermo Fisher Scientific, Inc.), and 0.2% of Epidermal Growth factor (EGF, PeproTech EC, UK) and Fibroblast Growth factor (FGF, Gibco, Thermo Fisher Scientific, Inc.). Using the trypan blue exclusion method and a Neubauer counting chamber, cells were counted and seeded at 50,000 cells/cm² in tissue culture-treated flasks (Falcon, Corning Inc., NY, USA). The culture was kept at 37°C in a humidified atmosphere of 5% CO₂. Cells were maintained up to 58 passages, at which point they were properly disposed of, while previously frozen cells were thawed.

Differentiating cells were initially cultured in tissue culture-treated plates (Falcon, Corning Inc., NY, USA) for 24 hours using NSC medium. Afterwards, the medium was replaced with neural differentiation inducing medium with Euromed-N medium supplemented with 0.5% of N-2, 1% of P/S, 1% of B-27 (Gibco, Thermo Fisher Scientific, Inc.) and 0.1% of FGF.

The N2a was also cultured in a monolayer, using a culture medium composed of equal parts Opti-MEM (Gibco, Thermo Fisher Scientific, Inc.) and a mix of D-MEM (Gibco, Thermo Fisher Scientific, Inc.) with 10% Fetal Bovine Serum (FBS, Gibco, Thermo Fisher Scientific, Inc.), 2% P/S and 2% Glutamine (Gibco, Thermo Fisher Scientific, Inc.). Cells were passaged in the same manner as NSCs the with exception of the use of 2 mL 0.1% Trypsin (Gibco, Thermo Fisher Scientific, Inc.) at 37°C for 3-4 minutes and then inactivated with medium containing FBS instead of Accutase.

2.2.1. Cells freezing and thawing

Cells were frozen in a mix of 90% medium and 10% dimethyl sulfoxide (DMSO, Merck, USA.) at 4,000,000/mL in a cryovial. The cryovials were then frozen at -80°C using a Mr. Frosty for stable temperature dropping. Contents of the cryovials were thawed at 37°C and seeded on a T-Flask. After cell adhesion (10-12 hours later) culture medium was changed to remove DMSO.

2.3. Viability assay

Cell viability was evaluated using the Guava Easycyte 5HT flow cytometer (Luminex Corp., Austin, Texas, USA), according to the manufacturer's specifications using cells seed into 12-well culture plates. All cells were collected from each individual well and resuspended in PBS. 40 µL of cell suspension was added to 110 µL of Guava Viacount® Reagent (Luminex Corp. Austin, Texas, USA). After five minutes of incubation the sample was analysed by the cytometer. Guava Suite Software (Luminex Corp. Austin, Texas, USA) was used to analyse the results.

2.4. *In vitro* neural injury models

To mimic oxidative stress and Parkinsonism in recipient cells, hydrogen peroxide (H₂O₂, 107209; MERCK) and 1-methyl-4-phenylpyridinium (MPP⁺, D048-000; MERCK) were used respectively. Cells were cultured in 12-well tissue culture-treated plates at a density of 47,500 cells/cm² for 24 hours prior exposure of several compound concentrations, 20 µm-10 mM for MPP⁺ and 50-500 µM for H₂O₂. After 24 hours of MPP⁺ or H₂O₂ exposure, cells were collected for cell viability assays.

2.5. 3D cell culture

The design and optimization protocol to establish 3D cultures of NSCs was performed in the laboratory of Prof. Joana Miranda, iMed-Lisboa, Faculty of Pharmacy. NSCs were first cultured on a 96-well Ultra Low Attachment Plate (Merck) to attest aggregation potential for up to five days using NSC medium exchanged every two days.

After propagation in 2D, cells were cultured as 3D aggregates in Spinner Flasks under two different conditions. In Condition 1, 1,000,000 cells/mL were seeded in culture medium with 5% of fetal bovine serum (FBS), whereas in Condition 2 we used 500,000 cells/mL and no FBS. In order to culture NSCs in Spinner Flasks, NSCs were first expanded in 2D until reaching a confluence of 80%. After detaching and counting, cells were suspended in medium that corresponded to 70% of the total volume, which translates to a concentration of 143%. The suspension went through 5 cycles of 15 minutes agitation and 5 minutes rest, and from then on kept at a constant agitation of 70 rpm. After 10-12 hours, the cell suspension was diluted to the final concentration of 100% by adding the remaining 30% of culture medium. The medium was

replaced 24 hours after inoculation without FBS nor PS and with half the concentration of FGF and EGF (previously validated in the laboratory). After 24 and 48 hours of inoculation, half of the total medium was replaced. 24 hours later, or 72 hours after inoculation, the media was again replaced and the culture was left undisturbed during the 48 hours of conditioning, after which the Conditioned Media (CM) was collected.

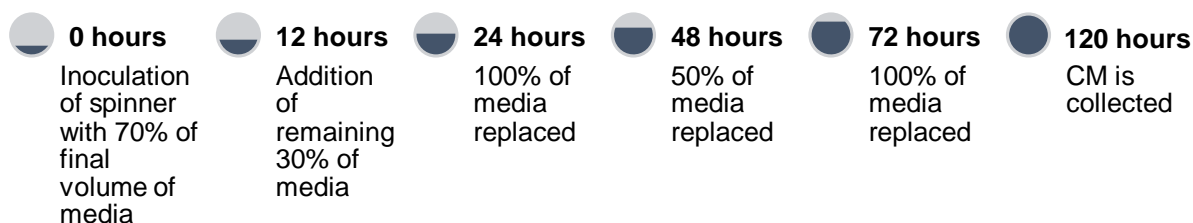


Figure 6 – Schematic representation of the protocol for NSC 3D-culture system using spinner flasks. The culture medium was fully replaced at 24 and 72 hours post inoculation and half of it was replaced at 48 hours post inoculation. The culture was left undisturbed for the last 48 hours.

2.5.1. Cell aggregate measurement

Samples of NSC aggregates were extracted throughout the aforementioned protocol to measure the size and stability of the NSC spheroids. To account for different dimensions across width and length, 3 measures offset by a 60° angle were taken in each aggregate, and the average was then considered. The size of the NSC aggregates was evaluated by Image Analysis using the ImageJ Software (public domain).

2.5.2. Paraffinization of neurospheres

To prepare NSC spheroids for immunocytochemistry analysis, samples were stabilized in paraffin. Then, collected samples were washed and fixed overnight in 4% solution of Paraformaldehyde (PFA). The fixed tissue was suspended in a solution of 2% agarose. After cooling, the agarose plug was dehydrated in increasingly higher concentrations of ethanol (70-100%) and then xylene. Finally, the plug was inserted into a histocassette, covered with paraffin at 60°C and cooled overnight at -20°C prior to sectioning. The paraffin block was cut into 10 µm thick slices in a microtome. The sections were mounted on slides (Merck) and kept at room temperature.

2.5.3. Haemotoxylin-eosin staining

The NSC spheroids were deparaffinized using 100% xylene and rehydrated using decreasing concentrations of ethanol (70-100%). The sections were stained for 20 minutes in Harris

Hematoxilin (HH S32, Sigma-Aldrich), washed with flowing tap water and then further stained for 2 minutes in Eosin stain (Sigma-Aldrich), which in turn was washed using distilled water. Afterwards, NSCs were again dehydrated using the aforementioned protocol, prior to mounting with Mowiol (Sigma-Aldrich).

2.6. Protein quantification

Protein quantification in both NSC culture systems led us to assure that 2D- and 3D-associated NSC secretome derived from the same number of cells and therefore could be compared. This quantification was performed using the Bradford Protein Assay. Firstly, a calibration curve was prepared by successive dilutions of Bovine Serum Albumin (BSA) in water. Then, 200 μ L of Bradford reagent (Bio-Rad Laboratories, USA) were added to each sample and properly homogenised. After 5 minutes, the absorbance was measured in a microplate reader (BMG Labtech, Ortenberg, Germany). Samples from 2D-cultured NSCs were used to generate the following calibration curve:

$$\text{Cell Concentration} = \frac{\text{Absorbance} - 0,3593}{0,0009}$$

This expression was then applied to the absorbance measured in samples from 3D cultured NSC, resulting in \sim 4.5 thousand cells per mL. After obtaining this result, it became possible to culture cells in 2D in an equivalent manner to the 3D and obtain two comparable sources of CM.

2.7. Secretome concentration

To avoid cell clogging, the collected CM was centrifuged at 500 *g* for 5 minutes to remove cells and aggregates. The Amicon® Ultra-Centrifugal Filter Unit (Merck) with a cut-off of 3 KDa was used, allowing the concentration of 15 mL of culture medium per centrifugal cycle. To operate the concentrator, the CM was pipetted to the sample reservoir and the concentrator was placed in the centrifuge, taking care to place the filters aligned with the radius of the device. The concentrators were then centrifuged at 2,700 *g* for 90 minutes, after which the filtrate was removed, and more CM was supplied. The concentrated medium was then removed from the sample reservoir and frozen at -80°C.

2.8. Total RNA extraction

Cells were collected, homogenized in 500 μ L Trizol (Thermo Fisher Scientific, Inc.) and stored at -80°C until processing. To extract RNA, 100 μ L of chloroform were added to the sample. After 15

minutes of centrifugation at 12,000 *g*, the aqueous phase was isolated, and the RNA was precipitated by the addition of 250 μ L of isopropanol. After another round of centrifugation, the supernatant was removed, and the pellet was washed with 75% ethanol. The sample was resuspended in water and finally quantified in a QuBit fluorometer (Thermo Fisher Scientific, Inc.).

2.9. qRT-PCR assay

The expression of several genes was investigated in NSCs by qRT-PCR. Firstly, the synthesis of the complementary DNA (cDNA) was achieved using the NZY First-Strand cDNA Synthesis Kit (NZYTech Lda., Lisbon, Portugal). According to the specifications, 1 μ g of RNA was diluted in 12.5 μ L of RNase free water. A 10% solution of DNase diluted in Buffer 10X was prepared and 1.5 μ L was added to the sample, which underwent a cycle of 20 minutes at 37°C and another of 10 minutes at 75°C to remove any remaining DNA contamination. To synthesize the cDNA, 3 μ L of random hexamers and dNTP's was added and the sample placed for 5 minutes in the thermocycler at 65°C. Finally, the reverse transcriptase and Reaction Buffer mix were added. The thermocycler was programmed thusly: 10 minutes at 25°C, 50 minutes at 50°C and 5 minutes at 85°C. The sample was then kept at -20°C until the next step. Each sample was diluted 1:1 in RNase-free water and 2 μ L of the sample were added to 5 μ L of Sybr Green (bio-92020; Biorline, London, UK), 0.4 μ L of each primer and 0.2 μ L of water. The analysis was performed in an Applied Biosystems® QuantStudio™ 7 Flex Real-Time PCR System (Applied Biosystems, Foster City, CA, USA) using the following cycle: 2 minutes at 50°C, 10 minutes at 95°C, followed by 30 steps of 95°C for 15 seconds and 60°C for 1 minute. To calibrate, the levels of gene expression were normalized to the housekeeping gene HPRT1.

Table 1 – List of primers used for qRT-PCR.

GENE	PRIMER FWD (5'- 3')	PRIMER REV (5'- 3')
<i>SOX2</i>	AGGGTTCTTGCTGGGTTTTGATTCT	CGGTCTTGCCAGTACTTGCTCTCA
<i>NESTIN</i>	CTCAGATCCTGGAAGGTGGG	GCAGAGTCCTGTATGTAGCCA
<i>BIII-TUBULIN</i>	GCGCCTTTGGACACCTATTCA	TCCGCACGACATCTAGGACTG
<i>MAP2</i>	G TTCAGGCCCACTCTCCTTC	CTTGCTGCTGTGGTTTTCCG
<i>GFAP</i>	CCAAACTGGCTGATGTCTACC	GCTTCATCTGCCTCCTGTCTA
<i>PGC-1A</i>	GGACATGTGCAGCCAAGACTCT	CACTTCAATCCACCCAGAAAGCT
<i>SOD2</i>	CAGACCTGCCTTACGACTATGG	CTCGGTGGCGTTGAGATTGTT
<i>HPRT1</i>	GGTGAAAAGGACCTCTCGAAGTG	ATAGTCAAGGGCATATCCAACAACA

2.10. Immunocytochemistry

Neurospheres were deparaffined and rehydrated using the same protocol for haematoxylin-eosin staining. The initial step of antigen retrieval was achieved using citrate buffer (Sodium Citrate 10 mM at pH 6.0) at 95-100°C for 15 minutes. The blocking solution used was 10% Donkey serum (D9663, Merck, USA) and 0.1% Triton x-100 in PBS. The samples were kept in blocking solution for 1 hour. Then, the primary antibodies diluted in blocking solution were added overnight at 4°C. After 3 washes with PBS, the secondary antibodies were incubated for 2 hours at room temperature, taking precautions to avoid exposure to light. After 3 washes, nuclei were stained with 0.1% Hoechst Nuclear staining (Thermo Fisher Scientific, Inc.) for 5 minutes. Finally, the samples were mounted using Mowiol and the resulting fluorescent signals were imaged using fluorescence microscopy assessments performed with a Zeiss AX10 microscope (Carl Zeiss Corp.), equipped with a 63x/1.4 oil plan-apochromat objective and an AxioCam HRm camera (Carl Zeiss Corp.).

Table 2 – List of primary antibodies used for immunohistochemistry.

TARGET	HOST	SOURCE	DILUTION
NESTIN	mouse	Merck Millipore Corp. (MAB353)	1:200
GFAP	mouse	Merck Millipore Corp. (MAB360)	1:200
MAP2	rabbit	Merck Millipore Corp. (AB5622)	1:500
KI-67	mouse	Merck Millipore Corp. (AB9260)	1:200

Table 3 – List of secondary antibodies used for immunohistochemistry.

TARGET	HOST	SOURCE	DILUTION
ALEXA 568	Anti-mouse	Invitrogen (A-10037)	1:200
DYLIGHT 488	Anti-rabbit	Abcam (AB 96883)	1:200

2.11. NSC-derived CM-based assays

To assess and compare the impact of NSC secretome on different target cells and injury models, a series of controls were established, namely a control without CM exposure, and a control with the same volume of non-conditioned concentrated medium (fresh medium). These different control conditions allow to evaluate the effect of two types of NSC-CMs, the 2D- and the 3D-derived CMs, each on at both 5x and 10x concentration. The exposure to MPP⁺ and H₂O₂ and CMs was performed in the same manner as the original injury models to make sure the cells were

in a comparable state of confluence before administering the toxic compounds. After 24 hours of incubation the cell viability was evaluated with the Guava ViaCount® assay.

2.12. Flow cytometry

The remaining cell samples from the CM-based assays were used to detect Bcl-2 expression by flow cytometry analysis. Cells were firstly fixed with 4% PFA at 4°C for 20 minutes. Afterwards, the samples were washed twice using a solution of 0.1% saponin in PBS. Between each step the samples were centrifuged, and the supernatant removed. Blocking was performed using PBS supplied with 0.25% saponin and 5% FBS for 20 minutes. After two rounds of washing, the primary antibody was incubated in a solution of 0.1% saponin and 5% FBS in PBS for 30 minutes at 4°C. The secondary antibody was diluted in the same mix for 30 minutes further. Finally, the samples were diluted in PBS with 2% FBS and the fluorescence signal was detected in the Guava EasyCyte Flow cytometer.

2.13. Statistical analysis

All results are presented as a mean ± Standard Error of the Mean (SEM). The SEM is calculated as follows:

$$SEM = \frac{\text{Standard Deviation}}{\sqrt{n}}$$

The statistical significance was determined by t-test, comparing a data set to the indicated control. A *p*-value lower than 0.05 was considered statistically significant, with additional emphasis placed on threshold indicated by the following subtitles: * for *p* < 0.05, ** for *p* < 0.005 and *** for *p* < 0.001.

3. Results and Discussion

3.1. Optimization of *in vitro* injury models in mouse neural stem cells and neural cells

To evaluate and compare the potential therapeutic effects of NSC secretome generated from different culture systems, it was initially necessary to develop a robust injured target model in NSCs as well as in other neural cell line. The selected toxic agents were MPP⁺, an inhibitor of mitochondrial complex I, which is used to mimic Parkinsonism in *in vitro* models [71], and H₂O₂, as a direct inducer of oxidative stress [118]. Therefore, and to avoid massive cell death, we began to incubate undifferentiated and differentiating NSCs, as well as N2a cells, with a wide range of different concentrations of both MPP⁺ and H₂O₂ for 24 hours and evaluated cell viability through the Guava ViaCount® assay (Figure 7-9). Of note, the dynamic of cell death levels, as a function of the toxic concentration, has been shown to resemble a sigmoidal curve [120]. Thus, by selecting values in the midrange, where the function is approximately linear, there was a minimal risk of reaching one of the plateaus where a fluctuation could more easily be missed [121]. In fact, after these experiments we were able to select one concentration of each toxic compound capable of inducing ~ 40-50% of cell death in the NSC and N2a cell line [119].

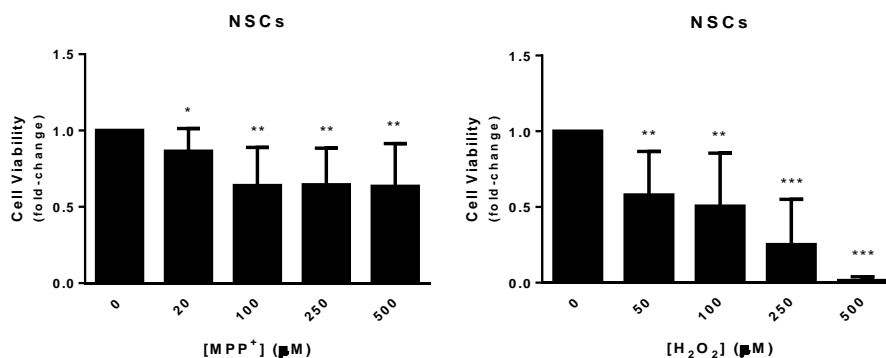


Figure 7 – MPP⁺ and H₂O₂ decrease cell viability in NSCs. The mouse NSC line NS-TGFP was expanded and treated for 24 hours with either MPP⁺ or H₂O₂ in self-renewal conditions, and then collected for cell viability analysis using the Guava ViaCount® assay. Ratio of live cells when compared with the total nucleated NSCs after exposure of several compound concentrations, MPP⁺ (left) or H₂O₂ (right). Data is expressed as mean ± SEM fold-change for at least 3 independent experiments. **p* < 0.05, ***p* < 0.01, ****p* < 0.001 from non-treated cells (control).

Curiously, our results have shown that differentiating NSCs were extremely resistant to cell death when compared with undifferentiated and self-renewing NSCs. This result appears to be caused by the overlap in the signalling pathways employed during differentiation and cell death [122, 123]. Due to the staggering amount of toxic necessary to induce injury, the creation of an injury model based on differentiating cells was shelved.

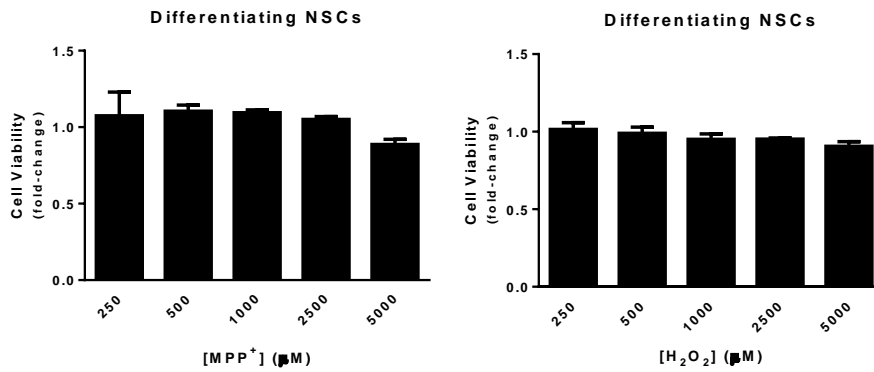


Figure 8 – MPP⁺ and H₂O₂ did not affect cell viability of differentiating NSCs. The mouse NSC line NS-TGFP was expanded and treated for 24 hours with either MPP⁺ or H₂O₂ in differentiation conditions, and then collected for cell viability analysis using the Guava ViaCount® assay. Ratio of live cells when compared with the total nucleated NSCs after exposure of several compound concentrations, MPP⁺ (left) or H₂O₂ (right). Data is expressed as mean ± SEM fold-change for at least 3 independent experiments. **p* < 0.05, ***p* < 0.01, ****p* < 0.001 from non-treated cells (control).

The N2a cell line, chosen to mimic more mature neural cells, behaved similarly to the undifferentiated NSCs, when exposed to the toxics, albeit requiring a higher dose to induce an equivalent effect.

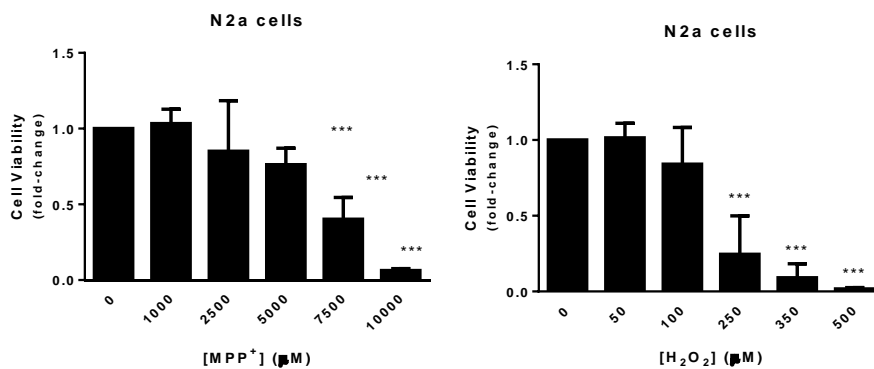


Figure 9 – MPP⁺ and H₂O₂ decrease viability of N2a cells. N2a cells were cultured for 24 hours and then treated with toxics for another 24 hours. Cells were then collected for cell viability analysis using the Guava ViaCount® assay. Cell viability after exposure to MPP⁺ (left) and H₂O₂ (right) is presented as mean ± SEM fold-change for at least 3 independent experiments. **p* < 0.05, ***p* < 0.01, ****p* < 0.001 from non-treated cells (control).

Thus, these initial experiments allowed us to select the concentration of 100 μM for both MPP^+ and H_2O_2 , in undifferentiated NSCs and of 250 μM for both MPP^+ and H_2O_2 in N2a cells, as it triggered the desired range of cell death without inducing significant morphological changes in both target cells.

3.2. Effect of NSC-derived secretome on MPP^+ and H_2O_2 -induced NSC death

Having established the injury target models, a proof-of-concept experiment was designed to test the initial hypothesis that the secretome of NSCs is beneficial and capable of inhibiting cell death in target neural cells, as well as to investigate whether our viability assay would be accurate enough to detect such effects. To that end, two batches of supplemented media were prepared. One batch was used to maintain NSCs in culture for 48 hours, therefore becoming enriched with the secretome of NSCs (conditioned medium, CM). The other batch was kept in an empty flask (without cells) and placed in the incubator for the same period of time (fresh medium, FM), to more closely resemble the conditions of the conditioned medium. These two supplemental media were used to supplement target NSC exposed to the previously selected cytotoxic agents. The medium supplementation of target cells was performed with either 25% or 50% of CM and FM (Figure 10, A and B).

In fact, although the addition of FM slightly increases cell viability in NSCs exposed to MPP^+ and H_2O_2 , the presence of CM induced a greater effect, indicating that some factor(s) secreted by NSCs induce a protective response on target injured NSCs.

The effect of the CM on the NSC beyond cell viability rescue was not assessed, however cells appeared to retain the same morphology, with no obvious phenotypic changes (data not shown).

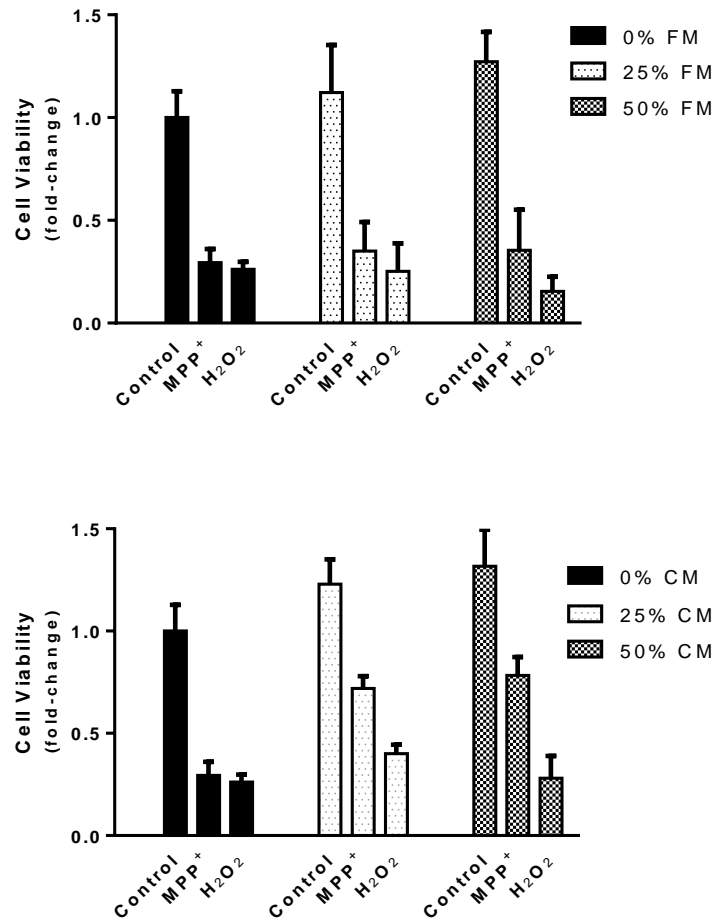


Figure 10 – NSC CM increases viability of injured target NSCs. NSCs were cultured for 24 hours and then treated with MPP⁺ or H₂O₂ and different percentages of fresh medium (FM) (*top*) or conditioned medium (CM) (*bottom*) for another 24 hours. Cells were then collected for cell viability analysis using the Guava ViaCount® assay. Cell viability is presented as mean ± SEM fold-change for at least 3 independent experiments.

Importantly, the effects induced by NSC secretome (CM) appeared to be more protective of cell death, rather than inducer of proliferation. In fact, in the absence of toxic exposure, the levels of cell viability were very similar between the CM and FM conditions. On the other hand, in the presence of MPP⁺ and H₂O₂, CM showed to be much more effective in preventing the decrease

in cell viability when compared with the FM. This effect was highlighted by presenting the ratio in cell viability between equivalent conditions supplemented with CM and FM (Figure 11).

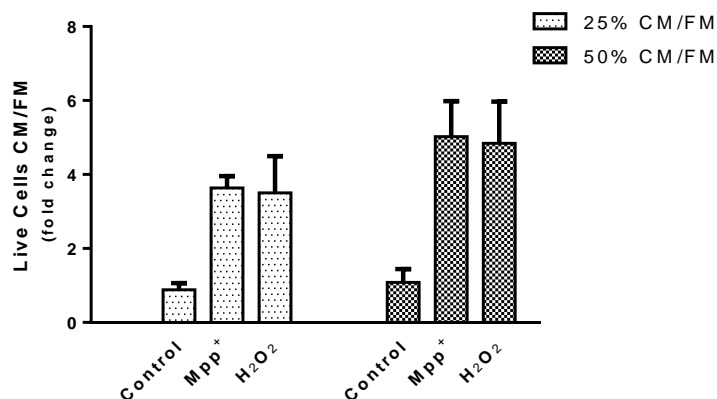


Figure 11 – NSC secretome increases viability of injured target NSCs. The results presented here represent the ratio between CM conditions-derived data with those obtained from FM conditions. Data is expressed as mean \pm SEM fold-change for at least 3 independent experiments.

3.3. Establishment of the NSC three-dimensional culture system for collection of NSC secretome

After testing the initial hypothesis, the next step was to develop a feasible 3D cultured system of NSCs to be able to compare the beneficial and therapeutic properties of CM collected from 2D and 3D cultured cells in the same previous injured models. These experiments were performed in collaboration with Prof. Joana Miranda in our Research Institute. Since it is easier to control 2D culture protocol, the 3D system was developed and optimized first, to latter adapt some details of the 2D culture protocol and match particular aspects such as the number of secretome-producing cells. For that, NSCs were cultured in ultra-low attachment plates (ULA plates) in a range of cell densities, with or without FBS which promote cell aggregation [108]. Although the conditions in a ULA plate do not directly translate into the conditions of the Spinner Flasks, they allowed a quick test regarding the NSC aggregation abilities as well as the stability of different sized aggregates for several days of culture (Figure 12).

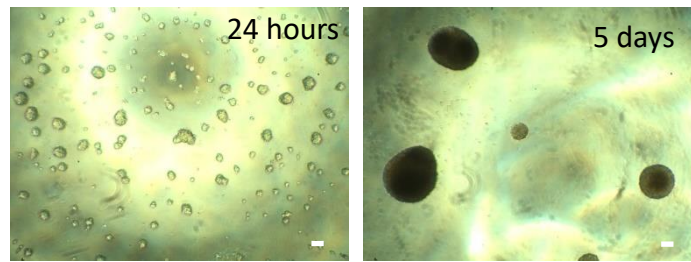


Figure 12 – Representative images of NSC aggregates grown in ULA plates. The cell condition presented consisted of a seeding of 50,000 cells and 5% of FBS, at 24 hours (left) and five days (right) after inoculation. Scale bar, 200 μm .

Subsequently, NSCs were cultured as aggregates in Spinner Flasks as previously described [108]. Initially, 2 different conditions were set up for a specific Spinner and controlled for 5 days, with regular sampling of the aggregates size. By the end of the protocol, it became apparent that the condition 1 resulted in aggregates disproportionately large, with diameters of 702 μm ($\sim 29 \mu\text{m}$, $n=9$) (Figure 13).

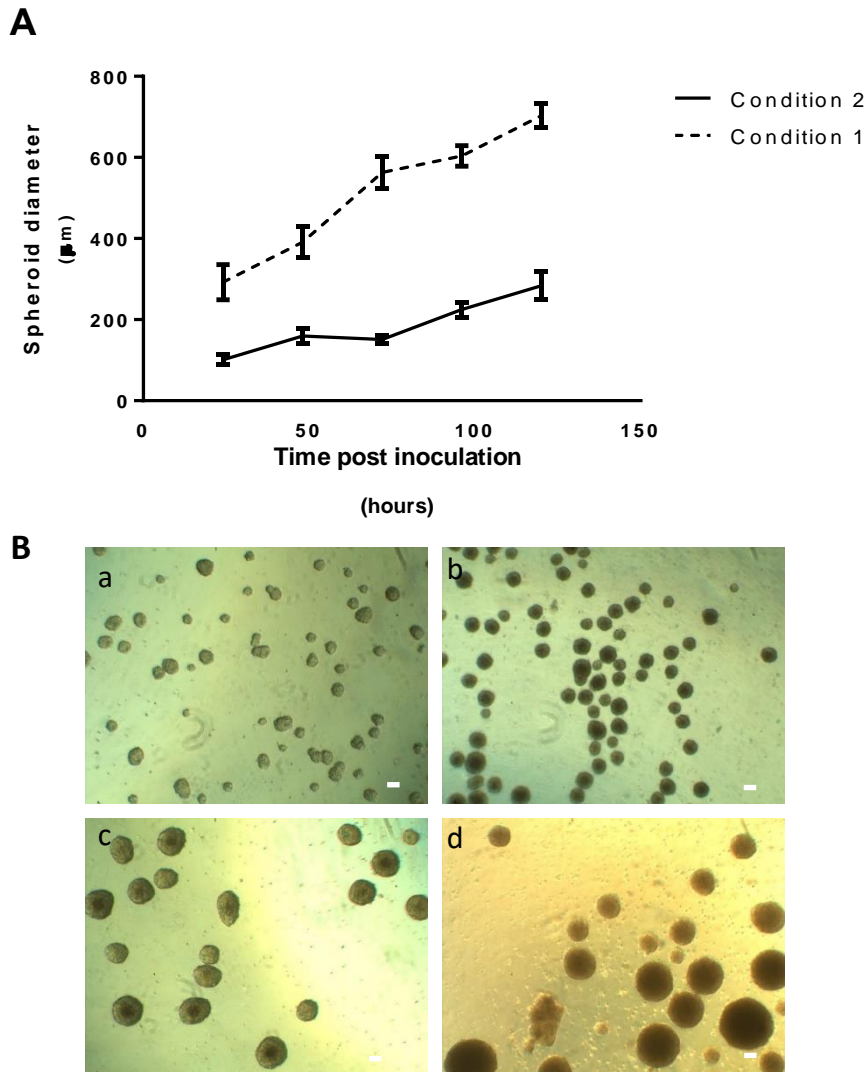


Figure 13 – Diameter of NSC spheroids increases throughout time. (A) Samples of NSC spheroids were collected during the protocol and measured. Data is expressed as mean \pm SEM for at least twenty-one independent measurements. (B) Representative images are presented for samples extracted from a condition 1 Spinner at 24 hours (a), 72 hours (b), 96 hours (c), and 120 hours (d) post inoculation.

To evaluate the presence or absence of necrotic centres in the NSC aggregates derived from Conditions 1 and 2, a staining with haematoxylin-eosin was performed on neurosphere slices. In fact, in contrast with the experimental Condition 1, Condition 2 did not exhibit the presence of necrotic centres (Figure 14).

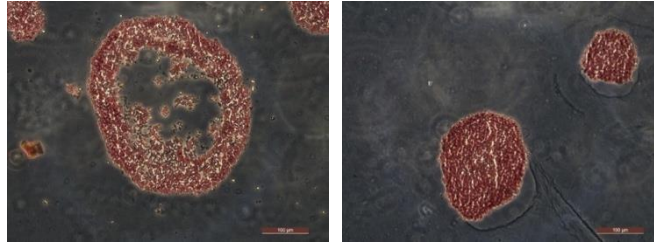


Figure 14 – Larger spheroids exhibit necrotic centres, whereas smaller spheroids are homogenous. Staining with haematoxylin-eosin on aggregates obtained after 6 days of culture from condition 1 (left), associated with higher initial cell density, displayed necrotic centres; whereas in condition 2 (right), associated with lower initial cell density, did not exhibit necrotic centres. Scale bar, 100 μm .

On the other hand, the larger aggregates found in Condition 1 exhibit necrotic centres, making it unfit for CM collection, as cell death normally results in increased release of cytokines that can negatively impact bordering cells [124]. Therefore, the experimental Condition 2 was selected as the best 3D culture system condition to maintain NSCs and collect NSC secretome for future experiments.

3.4. Comparison of the therapeutic impact of NSC secretome derived from 2D and 3D culture conditions

Since the method for obtaining 3D CM was established, it became necessary to design a 2D conditioning strategy that was comparable to the 3D. For that, we performed an assay of protein quantification to approximately match the concentration of secretome producing cells in both culture systems (Material and methods).

On the other hand, considering the high required volume of CM to collect, as well as the potential batch to batch variability, all CMs (2D and 3D-derived) were pooled prior to a concentrating step using Amicon Filter devices. Similarly, the same volume of FM was concentrated and prepared, as a control condition, since the concentration of proliferating and trophic factors present the culture medium could also induce protective effects *per se*. These concentrated CMs and FMs were then used to supplement for 24 hours the culture media of injured target NSCs and N2a neural cells, and the protective effect of the secretome in these different scenarios was re-evaluated.

Two different concentrations of CMs were tested for each type of CMs, 5X and 10X [108].

The results presented in Figure 15 represent the effect of CM vs the effect of FM, in each specific injury context. Interestingly, in undifferentiated NSCs, the addition of CM was beneficial across both toxic conditions. However, higher concentrations of CM did not correlate with higher live cell

counts, even showing a decreased effect. Moreover, in toxic conditions, 3D-derived CM appears to have a very mild improvement when compared with the 2D-derived CM.

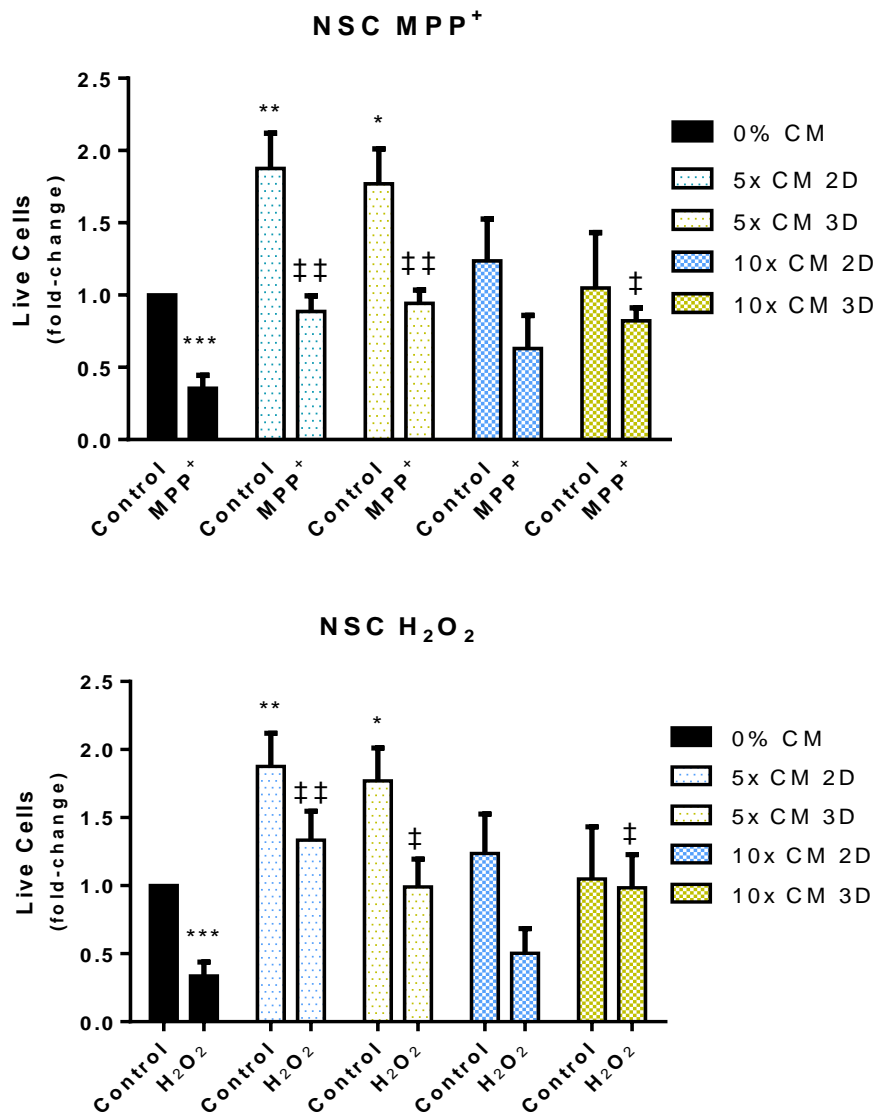


Figure 15 – NSC secretome increases cell viability of injury NSCs. NSCs were cultured for 24 hours and then treated with MPP⁺ or H₂O₂ and different percentages of 2D- or 3D-NSC conditioned medium (CM) for another 24 hours. Cells were then collected for cell viability analysis using the Guava ViaCount® assay. Cell viability is presented as mean ± SEM fold-change for at least 3 independent experiments. **p* < 0.05, ***p* < 0.01, ****p* < 0.001 from non-treated cells (control). †*p* < 0.05, ††*p* < 0.01 from cells treated with the corresponding toxic agent.

When we performed the same experiments but using N2a cells as target injured cells, an additional control condition was added. Incubation with FM allowed us to evaluate the effects of concentrated growth factors present in the culture medium on the viability of recipient cells. In

accordance with the results obtained in NSCs, the higher concentration of both CM and FM induced a negligible or negative impact in the survival levels of target cells in all conditions. In the N2a models, the effect of the CMs on injury was less visible and presented higher variability, particularly with respect to the MPP⁺ model. Nonetheless, the H₂O₂-induced injury of N2a suggests a trend similar to what was previously observed in NSC target cells in both injury models, namely a tendency to increase in viability when exposed to the various CMs. Once again, the 3D-derived CM did not appear to exhibit stronger therapeutic properties when compared with the 2D-derived NSC secretome.

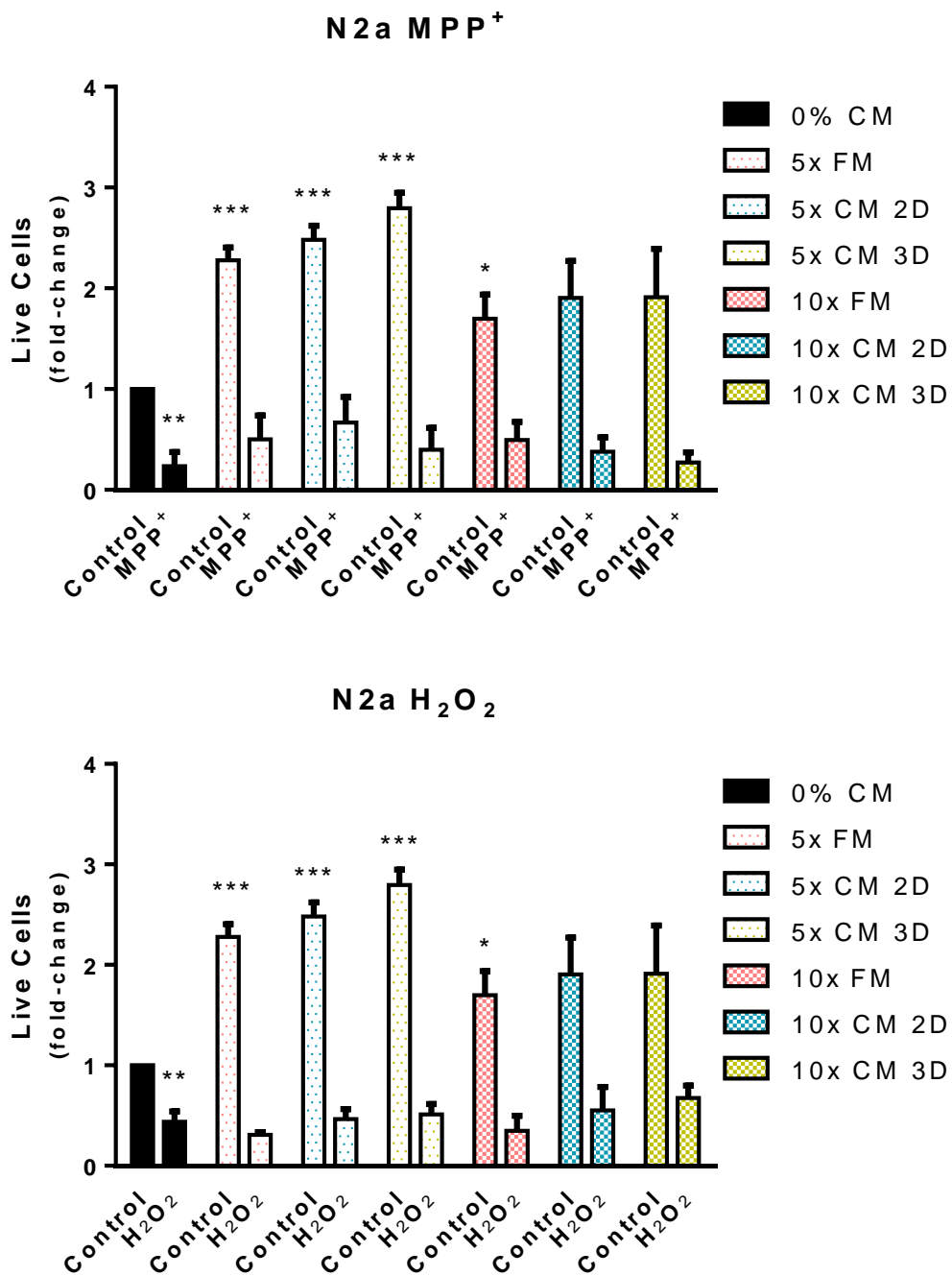


Figure 16 – NSC secretome did not affect cell viability of injury N2a cells. N2a cells were cultured for 24 hours and then treated with MPP⁺ or H₂O₂ and different percentages of fresh media (FM), 2D- or 3D-NSC conditioned medium (CM) for another 24 hours. Cells were then collected for cell viability analysis using the Guava ViaCount® assay. Cell viability is presented as mean ± SEM fold-change for at least 3 independent experiments. **p* < 0.05, ***p* < 0.01, ****p* < 0.001 from non-treated cells (control).

Thus, our results indicated that NSC-derived CM proved itself to be beneficial, displaying increased live cell count in the majority of injury conditions, when compared with the corresponding controls. In the case of NSC target cells, we observed a very consistent and robust effect of NSC-derived CMs in both injury models, indicating that this model of target cells is accurate and reproducible. In contrast, the use of N2a cell line as target cells did not show the same robustness, with high variability in the MPP⁺ injury model. Moreover, the fact that the N2a cell line is tumoral in origin, being derived from a neuroblastoma, may also be responsible for this lack of robustness. In addition, the little improvement of the therapeutic effect of 3D-derived CM when compared the 2D-derived CM, may partially rely on the presence of some cytokines associated with cell death. This, however, could be overcome in the future by further optimizing the cell bioreactor protocol

3.5. Molecular characterization of 2D- and 3D-derived NSCs

To confirm that the protective secretome was derived from naïve and multipotent NSCs, and not from a differentiated and heterogeneous cell population, we then evaluated and compared the cell fate of 2D- and 3D-secretome producing cells. In fact, whereas the stemness and multipotency of 2D cultured NSCs have been well described [125], the characterization of these new 3D-generated NSC spheres was not. Further, although the supplied culture medium was the same in 2D and 3D systems, it is known that mechanical alterations felt within cell spheroid structure interfere with the amount of growth factors uptake by NSCs along the radius of the aggregate, as well as with the activation of several cascade signalling pathways involved in differentiation [113, 117].

Thus, mRNA was extracted from both 2D- and 3D-derived NSCs, on the same time point of secretome collection, and qRT-PCR was performed to assess proliferation and differentiation markers (Figure 17, A-H). Regarding 3D-derived NSCs, mRNA was collected from the two previous tested spinner conditions. Indeed, despite the fact that the Condition 1 was dismissed, we would like to clarify how larger aggregates would interfere with differentiation levels.

Our results revealed profound changes between the 2D and 3D NSC populations, with 3D-derived NSCs showing high levels of cellular differentiation. In fact, SOX2, a key hallmark of undifferentiation [126], was significantly reduced in 3D-derived NSCs. Nestin, a marker of

undifferentiated NSCs was shown to be similarly expressed in 2D and 3D conditions. Indeed, since Nestin is also a marker for neural progenitor cells [127], it is not surprising that its expression may transiently co-exist with the presence of other differentiation markers. On the other hand, β III-tubulin, a marker of neuronal differentiation [128], and MAP2, a marker for mature neurons involved in the formation of microtubules and neurogenesis itself [129], were markedly upregulated in 3D-NSCs when compared with 2D NSCs. Regarding glial differentiation, our analysis showed that the gene expression of GFAP, a marker for astrocytes, was also markedly increased in 3D-derived NSCs, when compared with the monolayer system. Although FBS has already been shown to induce gliogenesis in other assays (data not shown), our data showed that NSCs derived from Condition 2 presented greater levels of this astroglial marker. Of note, the majority of differentiation markers were upregulated in Condition 2 when compared with Condition 1, which can be explained by the presence of necrotic centres, as cells were undergoing apoptosis instead of further progressing along the differentiating pathways.

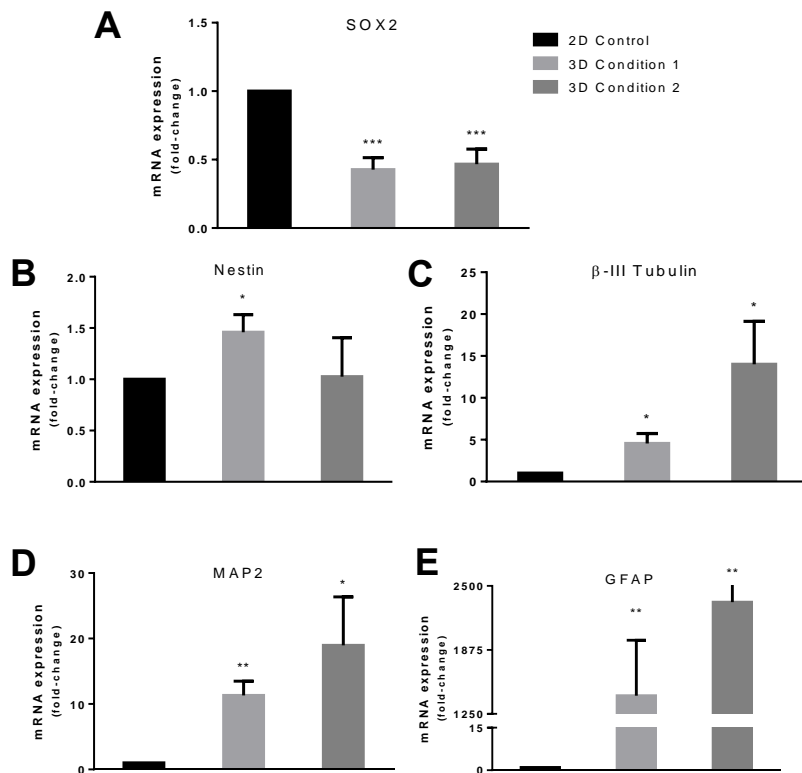


Figure 17 – Gene expression evaluated with qRT-PCR revealed increased differentiation in 3D cultured NSCs. NSCs were maintained in either 2D- or 3D-culture conditions in self-renewal conditions. Samples were extracted from the final day of culture, 48 hours for 2D-culture and 120 hours for 3D-culture for RT-PCR analysis to assess mRNA expression levels of the differentiation and proliferation markers. Effect of culture method on the expression levels of: **A** - SOX2, **B** – Nestin, **C** - β III-tubulin, **D** - MAP2 and **E** - GFAP. Values were normalized to the internal standard HPRT. Data is expressed as fold change over untreated NSCs. Data represent mean values \pm SEM for at least 3 independent experiments. * $p < 0.05$, ** $p < 0.01$, *** $p < 0.001$ from 2D NSCs (control).

In addition, since differentiation of stem cells has been associated with an increase of oxidative phosphorylation, we also assessed the expression levels of PGC-1 α and SOD2, the mitochondrial biogenesis inducer and the major scavenger of mitochondrial reactive oxygen species (ROS), respectively [130,131]. Our data validated the idea that cells present in 3D-derived NSCs are indeed under differentiation process, as undifferentiated NSC are known to depend mostly on glycolysis [131].

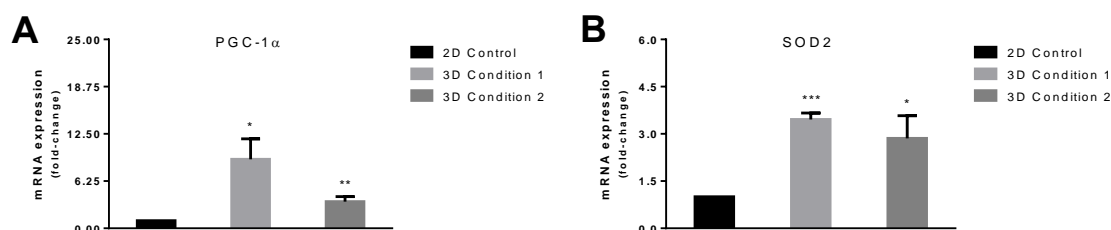


Figure 18 – Gene expression evaluated with qRT-PCR revealed increased mitochondrial activity on 3D-cultured NSCs. NSCs were maintained in either 2D- or 3D-culture conditions in self-renewal conditions for 48 and 120 hours respectively before being collected for RT-PCR analysis to assess mRNA expression levels of the mitochondria-related proteins. Effect of culture method on the expression levels of: **A** - SOX2, **B** – Nestin. Values were normalized to the internal standard HPRT. Data are expressed as fold change over untreated NSCs. Data represent mean values \pm SEM for at least 3 independent experiments. * $p < 0.05$, ** $p < 0.01$, *** $p < 0.001$ from 2D NSCs (control).

Lastly, to corroborate changes in mRNA of differentiation and stemness markers in NSC neurospheres, immunocytochemistry assays were performed for 3D-derived NSCs (Condition 2) (Figure 18, A-K) using antibodies against Nestin, MAP2, GFAP and Ki-67. Furthermore, this assay was performed to assess self-organization of the spheroid occurred, namely the distribution of cell populations with different fates. Firstly, our results corroborated the results obtained by qRT-PCR, by showing the presence of the high levels of differentiation markers. However, Nestin staining appeared tenuously, whereas MAP2 and GFAP markers were much more visible. Interestingly, the expression of the Ki-67 proliferation marker, albeit very lightly, was shown to be more peripheral along the neurospheres, suggesting that more proliferative cells were displayed along the surface of the spheroid. This result would be expected, as the surface of the spheroid has unfettered access to nutrients and oxygen.

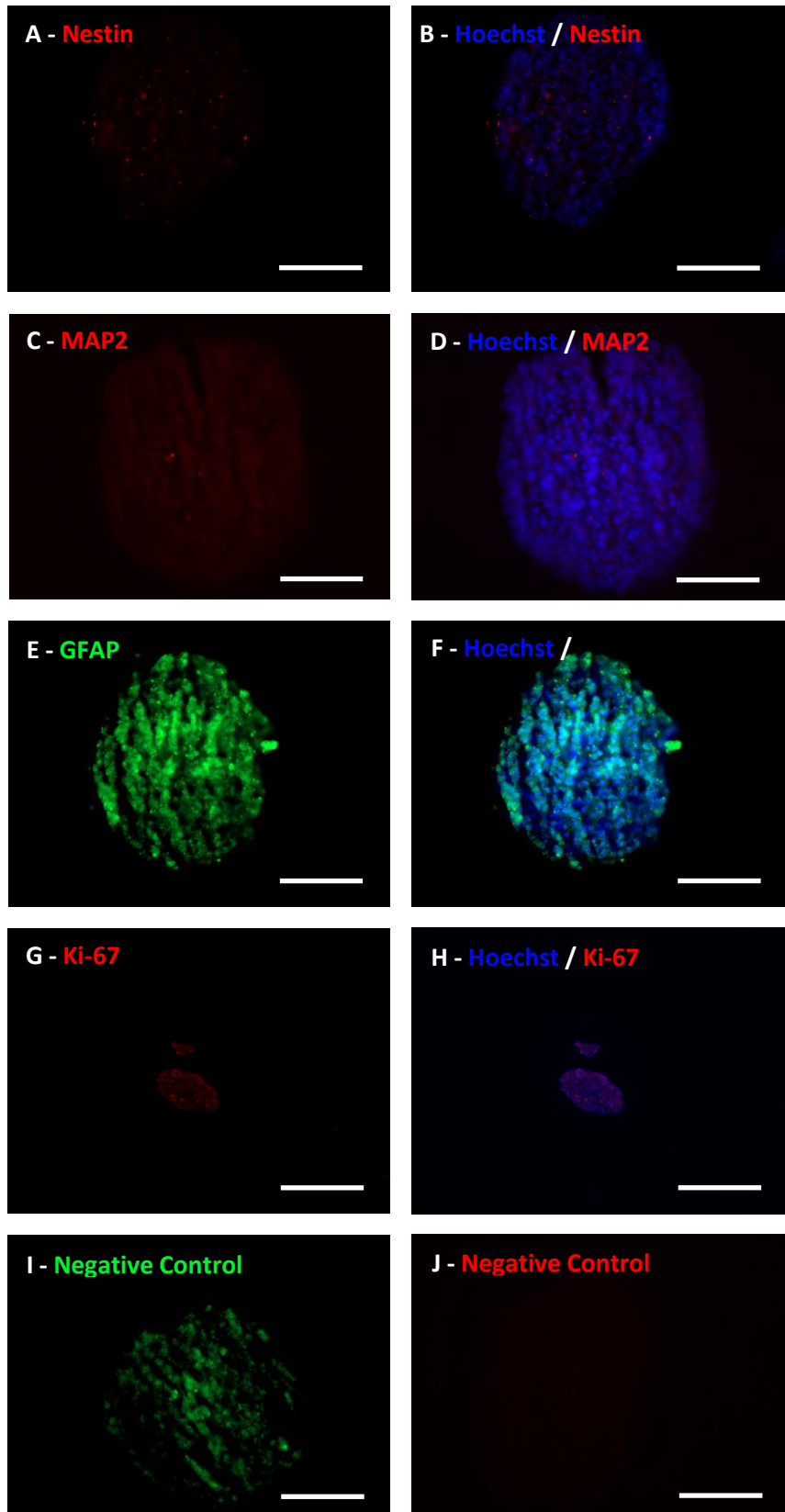


Figure 19 – Immunocytochemistry assays confirmed the expression of differentiation-related genes in the NSC spheroids. A, B - Staining with Nestin and Hoescht. C, D - Staining

with MAP2 and Hoesch. **E, F** - Staining with GFAP and Hoesch. **G, H** - Staining with Ki-67 and Hoescht. **I, K** - Staining only with secondary antibody, as a negative control (Dylight 488 and Alexa 568 respectively). Scale bar, 100 μm .

3.6. Molecular characterization of NSC secretome-receiving cells

Finally, in an effort to dissect some molecular changes in target cells that received NSC secretome, we decided to analyse Bcl-2 expression, an antiapoptotic protein of the Bcl-2 family member, in N2a target cells through Flow Cytometry (FC) analysis (Figure 19). Preliminary results suggested that NSC-derived CMs had no effect in Bcl-2 protein levels, independently of the CM concentration and the culture system of NSC producing secretome.

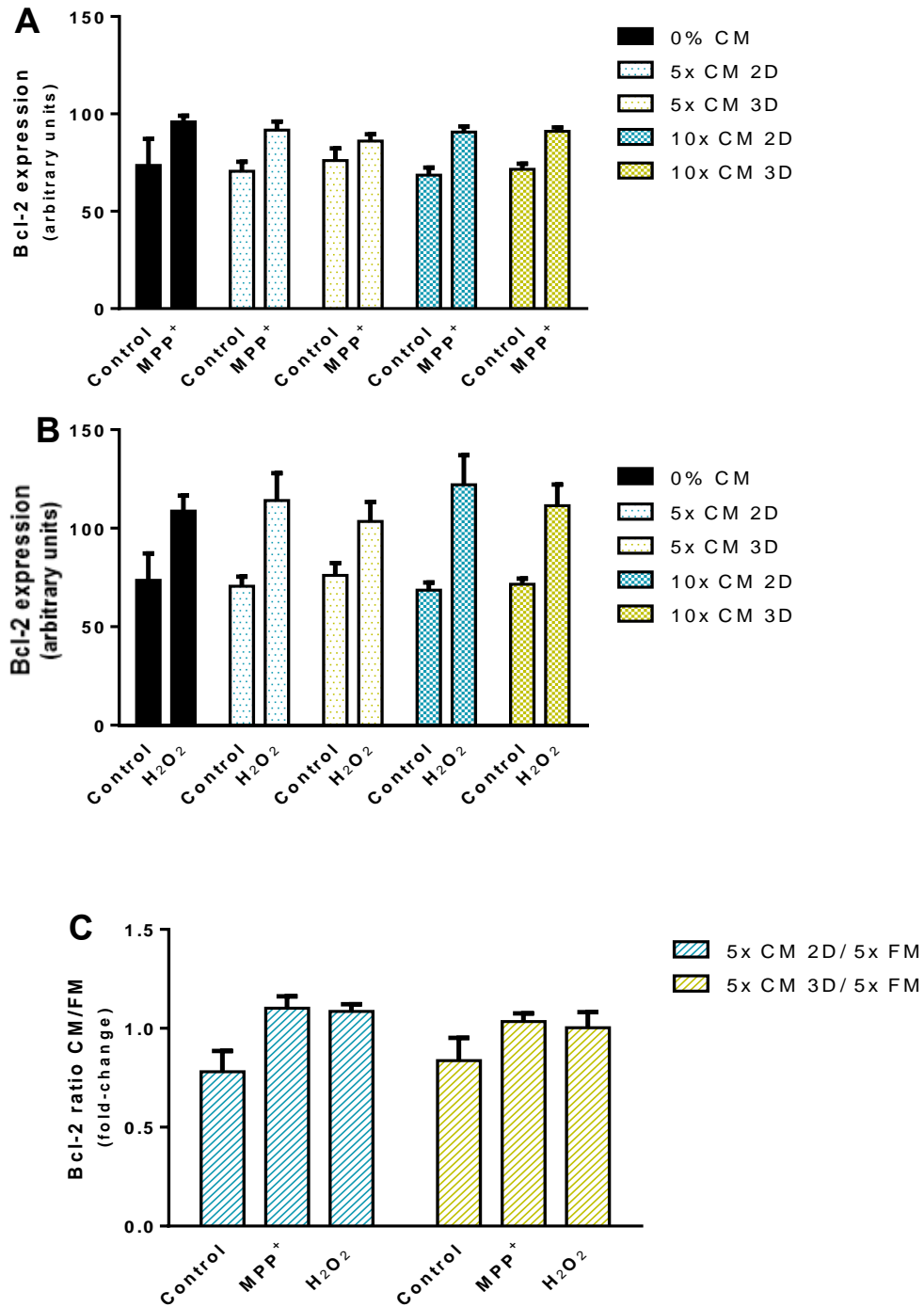


Figure 20 – Flow cytometry reveals no appreciable change in Bcl-2 expression following administration of CM in N2a injury model. A, B - Bcl-2 expression as measured (in arbitrary units) via Flow Cytometry, after removing a factor corresponding to the negative control, i.e. a sample with only the secondary antibody. C - Ratio of Bcl-2 expression between CM and FM conditions for 5x concentration. Data is expressed as mean \pm SEM fold-change for at least 3 independent experiments. * $p < 0.05$, ** $p < 0.01$, * $p < 0.001$ from non-treated cells (control).**

While this result may appear counterintuitive, it is possible that the protective effect is not related with this particular protein and may instead depend on another signalling pathway.

4. Conclusions and Future Perspectives

The question behind this project was two-fold: would NSC secretome have a positive effect on *in vitro* injury models of NSCs, and if so, how would different culture systems impact this effect? The proof-of-concept experiment quickly validated the paracrine hypothesis [99], showing that ordinary CM was enough to induce protection in models of oxidative stress and simulated Parkinsonism. This result was particularly important due to the relative ease of obtaining simple CM, with no optimization of the culture method, highlighting the importance of secretome as a potential therapy for neurodegenerative diseases. The following question pertained with how to guide cells towards the production of an improved secretome. To that end, and based on the protocol previously used in Prof. Miranda's laboratory [108], cells were cultured both as 3D aggregates and as a comparable monolayer culture, to compare the effects of the culture method on the NSC secretome. After testing both types of CMs, it became apparent that there was little improvement when 3D sourced CM was compared with 2D sourced CM. Moreover, the higher concentration of CM did not correlate with increased CM-protection on target injured cells. However, considering the lack of a thorough optimization step in the spinner protocol, it stands to reason that 3D culture resulted in the production of cytokines that induce cellular death. Furthermore, different CM concentrations should be also attempted, as the points tested appear to be outside of the linear portion of the dose-response curve [121].

Considering the framework of this experiment, there are also other parameters that could be tested in the future, namely the addition of a microdosage of toxic agents to the secretome producing NSCs, as a form of indirect conditioning of the secretome. This approach will possibly elicit an adaptative protective response from NSCs to neighbouring damaged cells.

On the other hand, qRT-PCR and immunohistochemistry assays showed that cells in 3D aggregates are no longer a homogeneously stem population, being instead in several stages of differentiation. While this was to be expected, it raised the question that the populations responsible for the production of secretome are fundamentally different. Thus, two paths are presented, on the one hand, it could be advantageous to optimize 3D culture regardless of NSC differentiation levels, considering only the best possible conditions of the secretome. This approach could even lead to the use of fully differentiated brain organoids, to assess the secretome producing capabilities of different brain regions, with particular interest in midbrain organoids, due to the dopaminergic neurons contained therein. While approach would better mimic the *in vivo* conditions it would also result in a very heterogeneous population masking the source of the beneficial CM components. On the other hand, the use of a pure population of NSCs would allow to isolate the beneficial components of the secretome and study their effects. Finally, it is of the utmost relevance a deep molecular analysis of the NSC-derived CM, both in terms of proteome and microRNA profile. Another factor that could provide interesting information pertains to the recipient cells, particularly to the alterations that these cells may exhibit in terms of metabolism and activated signalling pathways. Overall, this project lays a proverbial first stone in the study of the secretome of NSC in all its therapeutic potential. While there are numerous

avenues left to explore in order to improve and continue the project, the results that were achieved can support further experiments and optimizations in an effort to harness the clinical potential of NSC-sourced secretome.

5. References

1. _____Becker A, McCulloch E, and Till J. "Cytological Demonstration of the Clonal Nature of Spleen Colonies Derived from Transplanted Mouse Marrow Cells." *Nature* 197 (1963): 452–454
2. _____Nadig R R. "Stem cell therapy - Hype or hope? A review. " *Journal of Conservative Dentistry* 12.4 (2009): 131-138
3. _____Berger F, Gay E, Wion D, et al. "Development of gliomas: potential role of asymmetrical cell division of neural stem cells." *The Lancet Oncology* 5.8 (2004): 511-514
4. _____Zakrzewski W, Dobrzyński M, Szymonowicz M, et al. "Stem cells: past, present, and future." *Stem Cell Research & Therapy* 10.68 (2019)
5. _____Henrique D, Abranches E, Storey K G, et al. "Neuromesodermal progenitors and the making of the spinal cord." *Development* 142.17 (2015): 2864-2875
6. _____Tzouanacou E, Wegener A, Nicolas J F, et al. "Redefining the progression of lineage segregations during mammalian embryogenesis by clonal analysis." *Developmental Cell* 17.3 (2009): 365-76
7. _____Weiss M L, and Troyer D L. "Stem cells in the umbilical cord." *Stem Cell Reviews* 2.2 (2006): 155-162
8. _____Okita K, Ichisaka T, and Yamanaka S. "Generation of germline-competent induced pluripotent stem cells." *Nature* 448 (2007): 313-317
9. _____Hou P, Li Y, Deng H, et al. "Pluripotent Stem Cells Induced from Mouse Somatic Cells by Small-Molecule Compounds." *Science* 341.6146 (2013): 651-654
10. _____Zhao X, and Moore D L. "Neural stem cells: developmental mechanisms and disease modeling." *Cell and tissue research* 371.1 (2018): 1–6
11. _____Kazanis I, and ffrench-Constant C. "Extracellular matrix and the neural stem cell niche." *Developmental neurobiology* 71.11 (2011): 1006-1017
12. _____Tavazoie M, Van der Veken L, Doetsch F, et al. "A specialized vascular niche for adult neural stem cells." *Cell Stem Cell* 3.3 (2008): 279-288
13. _____Delgado A C, Ferrón S R, Fariñas I, et al. "Endothelial NT-3 delivered by vasculature and CSF promotes quiescence of subependymal neural stem cells through nitric oxide induction." *Neuron* 83.3 (2014): 572-85
14. _____Quiñones-Hinojosa A, Sanai N, Alvarez-Buylla A, et al. "Cellular composition and cytoarchitecture of the adult human subventricular zone: a niche of neural stem cells." *Journal of Comparative Neurology* 494.3 (2006): 415-34

- 15.____Curtis M A, Kam M, Eriksson P S, et al. "Human neuroblasts migrate to the olfactory bulb via a lateral ventricular extension." *Science* 315.5816 (2007): 1243-1249
- 16.____Tuncdemir S N, Lacefield C O, and Hen R. "Contributions of adult neurogenesis to dentate gyrus network activity and computations." *Behavioural Brain Research* 374.18 (2019)
- 17.____Riquelme P A, Drapeau E and Doetsch F. "Brain micro-ecologies: neural stem cell niches in the adult mammalian brain." *Philosophical transactions of the Royal Society of London. Series B, Biological sciences* vol. 363.1489 (2008): 123-137
- 18.____Bátiz L F, Castro M A, Wyneken, U, et al. "Exosomes as Novel Regulators of Adult Neurogenic Niches." *Frontiers in Cellular Neuroscience* 9.501 (2016)
- 19.____Ashton R S, Conway A, Schaffer D V, et al. "Astrocytes regulate adult hippocampal neurogenesis through ephrin-B signaling." *Nature Neuroscience* 15.10 (2012): 1399-406
- 20.____Sierra A, Abiega O, Neumann H, et al. "Janus-faced microglia: beneficial and detrimental consequences of microglial phagocytosis." *Frontiers in cellular neuroscience*. 7.6 (2013)
- 21.____Sierra A, Encinas J M, Maletic-Savatic M, et al. "Microglia shape adult hippocampal neurogenesis through apoptosis-coupled phagocytosis." *Cell Stem Cell* 7.4 (2010): 483-495
- 22.____De Simone R, Ajmone-Cat M A, Minghetti L, et al. "Apoptotic PC12 cells exposing phosphatidylserine promote the production of anti-inflammatory and neuroprotective molecules by microglial cells." *Journal of Neuropathology & Experimental Neurology* 62.2 (2003): 208-216
- 23.____Butovsky O, Koronyo-Hamaoui M, Schwartz M, et al. "Glatiramer acetate fights against Alzheimer's disease by inducing dendritic-like microglia expressing insulin-like growth factor 1." *Proceedings of the National Academy of Sciences of the United States of America* 103.31 (2006): 11784-11789
- 24.____Thored P, Heldmann U, Lindvall O, et al. "Long-term accumulation of microglia with proneurogenic phenotype concomitant with persistent neurogenesis in adult subventricular zone after stroke." *Glia* 57.8 (2009): 835-849
- 25.____Shen Q, Goderie S K, Temple S, et al. "Endothelial cells stimulate self-renewal and expand neurogenesis of neural stem cells." *Science* 304.5675 (2004): 1338-1340
- 26.____Udo H, Yoshida Y, Sugiyama H, et al. "Enhanced adult neurogenesis and angiogenesis and altered affective behaviors in mice overexpressing vascular endothelial growth factor 120." *Journal of Neuroscience* 28.53 (2008): 14522-14536
- 27.____Jin K, Zhu Y, Greenberg D A, et al. "Vascular endothelial growth factor (VEGF) stimulates neurogenesis in vitro and in vivo." *Proceedings of the National Academy of Sciences of the United States of America* 99.18 (2002): 11946-11950

28. Fabel K, Fabel K, Palmer T D, et al. "VEGF is necessary for exercise-induced adult hippocampal neurogenesis." *European Journal of Neuroscience* 18.10 (2003): 2803-2812
29. Nguyen N, Lee S B, Ahn J Y, et al. "Neuroprotection by NGF and BDNF against neurotoxin-exerted apoptotic death in neural stem cells are mediated through Trk receptors, activating PI3-kinase and MAPK pathways." *Neurochemical Research* 34.5 (2009): 942-951
30. Sairanen M, Lucas G, Castrén E, et al. "Brain-derived neurotrophic factor and antidepressant drugs have different but coordinated effects on neuronal turnover, proliferation, and survival in the adult dentate gyrus." *Journal of Neuroscience* 25.5 (2005): 1089-1094
31. Kim H, Li Q, Madri J A, et al. "Paracrine and autocrine functions of brain-derived neurotrophic factor (BDNF) and nerve growth factor (NGF) in brain-derived endothelial cells." *Journal of Biological Chemistry* 279.32 (2004): 33538-33546
32. Pencea V, Bingaman K D, Luskin M B, et al. "Infusion of brain-derived neurotrophic factor into the lateral ventricle of the adult rat leads to new neurons in the parenchyma of the striatum, septum, thalamus, and hypothalamus." *The Journal of Neuroscience: the official journal of the Society for Neuroscience* 21.17 (2001): 6706-6717
33. Ishitsuka K, Ago T, Kitazono T, et al. "Neurotrophin production in brain pericytes during hypoxia: a role of pericytes for neuroprotection." *Microvascular Research* 83.3 (2012): 352-359
34. Ottone C, Krusche B, Parrinello S, et al. "Direct cell-cell contact with the vascular niche maintains quiescent neural stem cells." *Nature Cell Biology* 16.11 (2014): 1045-1056
35. Spassky N, Merkle F T, Alvarez-Buylla A, et al. "Adult ependymal cells are postmitotic and are derived from radial glial cells during embryogenesis." *Journal of Neuroscience* 25.1 (2005): 10-8
36. Ramírez-Castillejo C, Sánchez-Sánchez F, Fariñas I, et al. "Pigment epithelium-derived factor is a niche signal for neural stem cell renewal." *Nature Neuroscience* 9.3 (2006): 331-339
37. Ferland R J, Batiz L F, Sheen V L, et al. "Disruption of neural progenitors along the ventricular and subventricular zones in periventricular heterotopia." *Human molecular genetics* 18.3 (2009): 497-516
38. Jiménez A J, García-Verdugo J M, Pérez-Fígares J M, et al. "Disruption of the neurogenic niche in the subventricular zone of postnatal hydrocephalic mice." *Journal of Neuropathology and Experimental Neurology* 68.9 (2009): 1006-1020
39. Roales-Buján R, Páez P, Jiménez A J, et al. "Astrocytes acquire morphological and functional characteristics of ependymal cells following disruption of ependyma in hydrocephalus." *Acta Neuropathologica* 124.4 (2012): 531-546
40. Shingo T, Gregg C, Weiss S, et al. "Pregnancy-stimulated neurogenesis in the adult female forebrain mediated by prolactin." *Science* 299.5603 (2003): 117-120

41. Mirescu C and Gould E. "Stress and adult neurogenesis." *Hippocampus* 16.3 (2006): 233-238
42. Snyder J S, Soumier A, Cameron H A, et al. "Adult hippocampal neurogenesis buffers stress responses and depressive behaviour." *Nature* 476.7361 (2011): 458-461
43. Katsimpardi L, Litterman N K, Rubin L L, et al. "Vascular and neurogenic rejuvenation of the aging mouse brain by young systemic factors." *Science* 344.6184 (2014): 630-634
44. Sawamoto K, Wichterle H, Alvarez-Buylla A, et al. "New neurons follow the flow of cerebrospinal fluid in the adult brain." *Science* 311.5761 (2006): 629-632
45. Bunn R, King W, Fowlkes J L, et al. "Early Developmental Changes in IGF-I, IGF-II, IGF Binding Protein-1, and IGF Binding Protein-3 Concentration in the Cerebrospinal Fluid of Children." *Pediatric Research* 58 (2005): 89–93
46. Shimazaki T, Shingo T and Weiss S. "The ciliary neurotrophic factor/leukemia inhibitory factor/gp130 receptor complex operates in the maintenance of mammalian forebrain neural stem cells." *The Journal of neuroscience: the official journal of the Society for Neuroscience* 21.19 (2001): 7642–7653
47. Sato K, Malchinkhuu E, Okajima F, et al. "HDL-like lipoproteins in cerebrospinal fluid affect neural cell activity through lipoprotein-associated sphingosine 1-phosphate." *Biochemical and Biophysical Research Communications* 359.3 (2007): 649-654
48. Berg D A, Belnoue L, Simon A, et al. "Neurotransmitter-mediated control of neurogenesis in the adult vertebrate brain." *Development (Cambridge, England)* 140.12 (2013): 2548–2561
49. Höglinger G U, Rizk P, Hirsch EC, et al. "Dopamine depletion impairs precursor cell proliferation in Parkinson disease." *Nature Neuroscience* 7.7 (2004): 726-735
50. Winner B, Desplats P, Winkler J, et al. "Dopamine receptor activation promotes adult neurogenesis in an acute Parkinson model." *Experimental Neurology* 219(2) (2009) 543-552
51. Brezun J M and Daszuta A. "Depletion in serotonin decreases neurogenesis in the dentate gyrus and the subventricular zone of adult rats." *Neuroscience* 89.4 (1999) 999-1002
52. Brezun J M and Daszuta A. "Serotonin may stimulate granule cell proliferation in the adult hippocampus, as observed in rats grafted with foetal raphe neurons." *European Journal of Neuroscience* 12.1 (2000): 391-396
53. Malberg J E, Eisch A J, Duman R S, et al. "Chronic antidepressant treatment increases neurogenesis in adult rat hippocampus." *Journal of Neuroscience* 20.24 (2000): 9104-9110
54. Jhaveri D J, Mackay E W, Bartlett P F, et al. "Norepinephrine directly activates adult hippocampal precursors via beta3-adrenergic receptors." *Journal of Neuroscience* 30.7 (2010): 2795-2806

55. Kulkarni V A, Jha S and Vaidya V A. "Depletion of norepinephrine decreases the proliferation, but does not influence the survival and differentiation, of granule cell progenitors in the adult rat hippocampus." *European Journal of Neuroscience* 16.10 (2002): 2008-2012
56. Waterhouse E G, An J J, Xu B, et al. "BDNF promotes differentiation and maturation of adult-born neurons through GABAergic transmission." *Journal of Neuroscience* 32.41 (2012): 14318-14330
57. Colditz M J, Catts V S, Coulson E J, et al. "p75 neurotrophin receptor regulates basal and fluoxetine-stimulated hippocampal neurogenesis." *Experimental Brain Research* 200.2 (2010): 161-167
58. Pinnock S B, Blake A M, Herbert J, et al. "The roles of BDNF, pCREB and Wnt3a in the latent period preceding activation of progenitor cell mitosis in the adult dentate gyrus by fluoxetine." *PLoS One* 5.10 (2010)
59. Dowding C H, Shenton C L and Salek S S. "A review of the health-related quality of life and economic impact of Parkinson's disease." *Drugs & Aging* 23.9 (2006): 693-721
60. Redgrave P, Rodriguez M, Obeso J A, et al. "Goal-directed and habitual control in the basal ganglia: implications for Parkinson's disease." *Nature Reviews Neuroscience* 11 (2010): 760-772
61. von Coelln R and Shulman L M. "Clinical subtypes and genetic heterogeneity: of lumping and splitting in Parkinson disease." *Current Opinion in Neurology* 29.6 (2016): 727-734
62. Weintraub D and Burn D J. "Parkinson's disease: the quintessential neuropsychiatric disorder." *Movement Disorders* 26.6 (2011): 1022-1031
63. Devine M J, Ryten M, Kunath T, et al. "Parkinson's disease induced pluripotent stem cells with triplication of the α -synuclein locus." *Nature Communications* 2.440 (2011)
64. Vargas K J, Makani S, Chandra S S, et al. "Synucleins regulate the kinetics of synaptic vesicle endocytosis." *Journal of Neuroscience* 34.28 (2014): 9364-9376
65. Bourdenx M, Koulakiotis N S, Tsiropoulos A, et al. "Protein aggregation and neurodegeneration in prototypical neurodegenerative diseases: Examples of amyloidopathies, tauopathies and synucleinopathies." *Progress in Neurobiology* 155 (2017): 171-193
66. Shahmoradian S H, Lewis A J, Lauer M E, et al. "Lewy pathology in Parkinson's disease consists of crowded organelles and lipid membranes." *Nature Neuroscience* 22 (2019): 1099-1109
67. Cremades N, Cohen S I A, Klenerman D, et al. "Direct Observation of the Interconversion of Normal and Toxic Forms of α -Synuclein." *Cell* 149.5 (2012): 1048-1059

68. Tyedmers J, Mogk A and Bukau, B. "Cellular strategies for controlling protein aggregation." *Nature Reviews Molecular Cell Biology* 11 (2010): 777–788
69. Chartier S and Duyckaerts C. "Is Lewy pathology in the human nervous system chiefly an indicator of neuronal protection or of toxicity?" *Cell Tissue Research* 373.1 (2018): 149-160
70. Michel P P, Hirsch E C and Hunot S. "Understanding Dopaminergic Cell Death Pathways in Parkinson Disease." *Neuron* 90.4 (2016): 675-691
71. Przedborski S, Tieu K, Vila M, et al. "MPTP as a mitochondrial neurotoxic model of Parkinson's disease." *Journal of Bioenergetics and Biomembranes* 36.4 (2004): 375-379
72. Schapira A H V, Cooper J M, Marsden C D, et al. "Mitochondrial Complex I Deficiency in Parkinson's Disease" *Journal of neurochemistry* 54.3 (1990): 823-827
73. Langston J W, Langston E B and Irwin I. "MPTP-induced parkinsonism in human and non-human primates--clinical and experimental aspects." *Acta Neurologica Scandinavica. Supplementum* 100 (1984): 49-54
74. Ferreira M and Massano J. "An updated review of Parkinson's disease genetics and clinicopathological correlations." *Acta Neurologica Scandinavica* 135.3 (2017): 273-284
75. Narendra D, Walker J E and Youle R. "Mitochondrial quality control mediated by PINK1 and Parkin: links to parkinsonism." *Cold Spring Harbor Perspectives in Biology* 4.11 (2012)
76. Deas E, Wood N W and Plun-Favreau H. "Mitophagy and Parkinson's disease: The PINK1–parkin link." *Biochimica et Biophysica Acta - Molecular Cell Research* 1813.4 (2011): 623-633
77. Anglade P, Vyas S, Agid Y, et al. "Apoptosis and autophagy in nigral neurons of patients with Parkinson's disease." *Histology and Histopathology* 12.1 (1997): 25-31
78. Van Laar V S and Berman S B. "The interplay of neuronal mitochondrial dynamics and bioenergetics: Implications for Parkinson's disease." *Neurobiology of Disease* 51 (2013): 43-55
79. Martin L J, Pan Y, Lee MK, et al. "Parkinson's disease alpha-synuclein transgenic mice develop neuronal mitochondrial degeneration and cell death." *Journal of Neuroscience*. 26.1 (2006): 41-50
80. Kamp F, Exner N, Haass C, et al. "Inhibition of mitochondrial fusion by α -synuclein is rescued by PINK1, Parkin and DJ-1." *EMBO Journal* 29.20 (2010): 3571-3589
81. Lindvall O, Brundin P, Marsden C D, et al. "Grafts of fetal dopamine neurons survive and improve motor function in Parkinson's disease." *Science* 247.4942 (1990) 574-5777
82. Hagell P and Brundin P. "Cell Survival and Clinical Outcome Following Intrastratial Transplantation in Parkinson Disease." *Journal of Neuropathology & Experimental Neurology* 60.8 (2001): 741–752

83. _____ Signer R A J, and Morrison S J. "Mechanisms that Regulate Stem Cell Aging and Life Span" *Cell Stem Cell* 12.2 (2013): Pages 152-165
84. _____ Takagi Y, Takahashi J, Hashimoto N, et al. "Dopaminergic neurons generated from monkey embryonic stem cells function in a Parkinson primate model." *Journal of Clinical Investigation* 115.1 (2005): 102-109
85. _____ Redmond Jr. D E, Bjugstad K B, Snyder E Y, et al. "Behavioral improvement in a primate Parkinson's model is associated with multiple homeostatic effects of human neural stem cells." *Proceedings of the National Academy of Sciences of the United States of America* 104.29 (2007): 12175–12180
86. _____ Wernig M, Zhao J P, Jaenisch R, et al. "Neurons derived from reprogrammed fibroblasts functionally integrate into the fetal brain and improve symptoms of rats with Parkinson's disease." *Proceedings of the National Academy of Sciences of the United States of America* 105.15 (2008): 5856–5861
87. _____ Bradley J A, Bolton E M and Pedersen R A. "Stem cell medicine encounters the immune system." *Nature Reviews Immunology* 2.11 (2002): 859-871
88. _____ Zhang M, Wang L, Sun Y, et al. "Lower genomic stability of induced pluripotent stem cells reflects increased non-homologous end joining." *Cancer Communications* 38.49 (2018)
89. _____ Itakura G, Kawabata S, Okano H, et al. "Fail-Safe System against Potential Tumorigenicity after Transplantation of iPSC Derivatives" *Stem Cell Reports* 8.3 (2017): 673-684
90. _____ Doi D, Morizane A, Takahashi J, et al. "Prolonged maturation culture favors a reduction in the tumorigenicity and the dopaminergic function of human ESC-derived neural cells in a primate model of Parkinson's disease." *Stem Cells* 30.5 (2012): 935-945
91. _____ Pluchino S, Cusimano M, Martino G, et al. "Remodelling the injured CNS through the establishment of atypical ectopic perivascular neural stem cell niches." *Archives Italiennes de Biologie* 148.2 (2010) : 173-183
92. _____ Willis C M, Nicaise A M, Pluchino S, et al. "The neural stem cell secretome and its role in brain repair." *Brain Research* 1729 (2020)
93. _____ Zhang J, Li Y, Chopp M. "Bone marrow stromal cells reduce axonal loss in experimental autoimmune encephalomyelitis mice." *Journal of Neuroscience Research* 84.3 (2006): 587-595
94. _____ Scuteri A, Casetti A and Tredici G. "Adult mesenchymal stem cells rescue dorsal root ganglia neurons from dying." *Brain Research* Volume 1116.1 (2006): 75-81
95. _____ Munoz J R, Stoutenger B R, Prockop D J, et al. "Human stem/progenitor cells from bone marrow promote neurogenesis of endogenous neural stem cells in the hippocampus of mice." *Proceedings of the National Academy of Sciences of the United States of America* 102.50 (2005): 18171–18176

96. ____ Crigler L, Robey R C, Phinney D G, et al. "Human mesenchymal stem cell subpopulations express a variety of neuro-regulatory molecules and promote neuronal cell survival and neurogenesis." *Experimental Neurology* 198.1 (2006): 54-64
97. ____ Mark Richardson R, Broaddus W C, Fillmore H L, et al. "Grafts of adult subependymal zone neuronal progenitor cells rescue hemiparkinsonian behavioral decline." *Brain Research* 1032.1 (2005): 11-22
98. ____ Tang Z, Yu Y, Zhou J, et al. "Induction of tyrosine hydroxylase expression in rat fetal striatal precursor cells following transplantation." *Neuroscience letters* 324.1 (2002): 13-16
99. ____ Mendes Pinheiro B, Teixeira F, Salgado A, et al. "Secretome of Undifferentiated Neural Progenitor Cells Induces Histological and Motor Improvements in a Rat Model of Parkinson's Disease." *STEM CELLS Translational Medicine* 7.11 (2018)
100. ____ Safi R, Gardaneh M, Gharib E, et al. "Optimized Quantities of GDNF Overexpressed by Engineered Astrocytes Are Critical for Protection of Neuroblastoma Cells Against 6-OHDA Toxicity." *Journal of Molecular Neuroscience* 46.3 (2012): 654-665
101. ____ He A, Jiang Y, Wang J A, et al. "The antiapoptotic effect of mesenchymal stem cell transplantation on ischemic myocardium is enhanced by anoxic preconditioning." *Canadian Journal of Cardiology* 25.6 (2009): 353-358
102. ____ Duval K, Grover H, Chen Z, et al. "Modeling Physiological Events in 2D vs. 3D Cell Culture." *Physiology (Bethesda)* 32.4 (2017):266-277
103. ____ Haycock J W. "3D cell culture: a review of current approaches and techniques." *Methods in Molecular Biology* 695 (2011): 1-15
104. ____ Burdick J A and Vunjak-Novakovic G. "Engineered microenvironments for controlled stem cell differentiation." *Tissue Engineering Part A* 15.2 (2009): 205-219
105. ____ Vergani L, Grattarola M and Nicolini C. "Modifications of chromatin structure and gene expression following induced alterations of cellular shape." *The International Journal of Biochemistry & Cell Biology* 36.8 (2004): 1447-1461
106. ____ Edmondson R, Broglie J J, Yang L, et al. "Three-dimensional cell culture systems and their applications in drug discovery and cell-based biosensors." *Assay and Drug Development Technologies* 12.4 (2014): 207-18
107. ____ McKee C and Chaudhry G R. "Advances and challenges in stem cell culture." *Colloids and Surfaces B: Biointerfaces* 159 (2017): 62-77
108. ____ Santos J M, Camões S P, Miranda J P, et al. "Three-dimensional spheroid cell culture of umbilical cord tissue-derived mesenchymal stromal cells leads to enhanced paracrine induction of wound healing." *Stem Cell Research Therapy* 6.90 (2015)

109. Khaitan D, Chandna S, Dwarakanath B S, et al. "Establishment and characterization of multicellular spheroids from a human glioma cell line; Implications for tumor therapy." *Journal of Translational Medicine* 4.12 (2006)
110. Gaedtke L, Thoenes L, Wagner E, et al. "Proteomic analysis reveals differences in protein expression in spheroid versus monolayer cultures of low-passage colon carcinoma cells." *Journal of Proteome Research* 6.11 (2007):4111-4118
111. Baker B M and Chen C S. "Deconstructing the third dimension: how 3D culture microenvironments alter cellular cues." *Journal of Cell Science* 125.13 (2012): 3015-3024.
112. Lin R Z and Chang H Y. "Recent advances in three-dimensional multicellular spheroid culture for biomedical research." *Biotechnology Journal* 3.9-10 (2008): 1172-1184
113. Eiraku M, Watanabe K, Sasai, Y, et al. "Self-Organized Formation of Polarized Cortical Tissues from ESCs and Its Active Manipulation by Extrinsic Signals." *Cell Stem Cell* 3 (2008): 519-532
114. Eiraku M, Takata N, Sasai Y, et al. "Self-organizing optic-cup morphogenesis in three-dimensional culture." *Nature* 472 (2011): 51-56
115. Velasco S, Paulsen B and Arlotta P. "3D Brain Organoids: Studying Brain Development and Disease outside the Embryo." *Annual Review of Neuroscience* 43 (2020): 375-389
116. Lancaster M, Renner M and Knoblich J A, et al. "Cerebral organoids model human brain development and microcephaly." *Nature* 501 (2013): 373–379
117. Faustino Martins J-M, Fischer C, Gouti M, et al. "Self-Organizing 3D Human Trunk Neuromuscular Organoids." *Cell Stem Cell* 26.2 (2020): 172-186
118. Guo Y-L, Chakraborty S, Huang F, et al. "Effects of Oxidative Stress on Mouse Embryonic Stem Cell Proliferation, Apoptosis, Senescence, and Self-Renewal." *Stem Cells and Development* 19.9 (2010)
119. Xiaoyun S, Ji-Hye J, Stary C M, et al. "Stem Cell-Derived Exosomes Protect Astrocyte Cultures From in vitro Ischemia and Decrease Injury as Post-stroke Intravenous Therapy." *Frontiers in Cellular Neuroscience* 13.394 (2019)
120. Santos L C, Vogel R, Meyer P, et al. "Mitochondrial origins of fractional control in regulated cell death." *Nature Communications* 10.1313 (2019)
121. Boncler M, Golanski J, Watala C, et al. "A new approach for the assessment of the toxicity of polyphenol-rich compounds with the use of high content screening analysis." *PloS one* 12.6 (2017)
122. Yi C H and Yuan J. "The Jekyll and Hyde functions of caspases." *Developmental Cell* 161 (2009): 21–34.

123. Solá S, Morgado A L and Rodrigues C M P. "Death receptors and mitochondria: Two prime triggers of neural apoptosis and differentiation." *Biochimica et Biophysica Acta - General Subjects* 1830.1 (2013): 2160-2166
124. Martin S J. "Cell death and inflammation: the case for IL-1 family cytokines as the canonical DAMPs of the immune system." *The FEBS Journal* 283.14 (2016): 2599-2615
125. Ribeiro M F, Genebra T, Solá S, et al. "Amyloid β Peptide Compromises Neural Stem Cell Fate by Irreversibly Disturbing Mitochondrial Oxidative State and Blocking Mitochondrial Biogenesis and Dynamics." *Molecular Neurobiology* 56.6 (2019): 3922–3936
126. Kashyap V, Rezende N C, Mongan N P, et al. "Regulation of stem cell pluripotency and differentiation involves a mutual regulatory circuit of the NANOG, OCT4, and SOX2 pluripotency transcription factors with polycomb repressive complexes and stem cell microRNAs." *Stem cells and development*, 18.7 (2009): 1093–1108
127. Park D, Xiang A P, Zhang L, et al. "Nestin Is Required for the Proper Self-Renewal of Neural Stem Cells." *Stem Cells* 28.12 (2010): 2162-2171
128. Tischfield M A, Baris H B, Engle E C, et al. "Human TUBB3 Mutations Perturb Microtubule Dynamics, Kinesin Interactions, and Axon Guidance." *Cell Volume* 140.1 (2010): 74-87
129. Dehmelt L and Halpain S. "The MAP2/Tau family of microtubule-associated proteins." *Genome Biology* 7.6 (2005)
130. Chen S D, Yang D I, Chuang Y C, et al. "Roles of oxidative stress, apoptosis, PGC-1 α and mitochondrial biogenesis in cerebral ischemia." *International Journal of Molecular Sciences* 12.10 (2011): 7199-7215
131. Bifari F, Dolci S, Decimo I, et al. "Complete neural stem cell (NSC) neuronal differentiation requires a branched chain amino acids-induced persistent metabolic shift towards energy metabolism." *Pharmacological Research* 158 (2020)